東海大學

資訊工程研究所

碩士論文

指導教授：黃育仁 博士

磁振造影之3D乳房區域切割輪廓描繪

Precise three-dimensional segmentation for breast region on Magnetic Resonance Imaging

研究生：劉子堉

中 華 民 國 一 零 五 年 七 月

Precise three-dimensional segmentation for breast region on Magnetic Resonance Imaging

Advisor

Prof. Yu-Len Huang

Department of Computer Science of

Tunghai University

Submitted in Partial Fulfillment

of the Requirements for the Degree

of Master of Engineering

by

IVPL

July 2016

東海大學碩士學位論文考試審定書

東海大學資訊工程學系 研究所

研究生 劉 子 堉 所提之論文

磁振造影之3D乳房區域切割輪廓描繪

經本委員會審查，符合碩士學位論文標準。

學位考試委員會

召 集 人 王經篤 簽章

委 員 張守富

黃貴12

指 導 教 授 黃貴12 簽章

中華民國 105 年 7 月 5 日

摘要

對於電腦輔助分析系統而言，在乳房磁振造影（MRI）上進行乳房區域輪廓描繪，是一個相當重要的步驟，準確的乳房體積已被醫生證實對其手術是有幫助的。在手術過程中，醫生必須用他們的經驗去估算他們所摘除的乳房組織體積，並且再將同等重量的鹽水袋或是矽膠放回體內。因此，自動乳房區域切割可以協助醫生在手術中快速的作出正確的決定。然而在自動化的乳房區域切割法中，最困難的部分是在於乳頭區域剃除或是留存，隨著乳房磁振造影越來越普遍的被使用，提升了自動化的乳房區域切割法的重要性以及臨床上的應用，為了達到這個目的，本研究實作了一個精確的自動化乳房區域切割方法，並且將其切割完的每一張影像分別記錄下來，用以計算整個乳房的體積。在研究提出的方法中，藉由前處理除去大量的雜訊，但是仍然保留了乳房的形狀，接著透過水平以及垂直投影，以提取出有興趣的部分(Region of interest)，即為左右乳房的區域，本研究測試評估十二個病例，實驗結果顯示該方法可以精確的描繪出乳房區域的輪廓。

關鍵字： 乳癌，磁振造影，影像切割，垂直與水平投影

ABSTRACT

Contouring of breast region is an important step in computer aided analysis of magnetic resonance imaging (MRI). The volume of breast region is helpful to physician in surgical operation. During the operation, physicians have to estimate the volume of the breast they removed by experience, then put the same weight of normal saline bag or silica gel in human body. Automatic contouring for breast region may assist physicians in making correct decision at surgical operation. However, automatic segmentation is difficult due to there are several resembled tissues around the breast region on MRI images. As breast MRI becomes more widespread used, a functional automatic contouring method is essential and its clinical application is becoming urgent. For this purpose, this study presents a precise method to segment the breast region on each image slice. Then the obtained contour is used to estimate the volume of the breast. The pre-processing of proposed method reduces plenty of noises but still preserves the shape of breast. By using horizontal and vertical projection to extract the region of interest (ROI), the proposed method could obtain a precise contour of breast region.

Keywords*:* breast cancer; breast MRI; image segmentation; horizontal and vertical projection

致謝

這篇論文的完成，首先要感謝的是我的指導教授黃育仁教授，在研究所這兩年內訓練我各項能力，讓我可以獨立思考、分析、解決問題。並且在課餘之時給予我鼓勵以及關心。在最後的論文寫作期間，老師也給我許多建議跟幫助，讓我可以如期完成我的論文。

也要感謝特地抽空前來參加的口試委員們：王經篤老師、張永昌老師，鼓勵並且認同我在於乳房區域切割上的貢獻，在口試完之後給予我寶貴的建議，讓我的論文可以更加完善。

再者我要感謝實驗室的學長姐，在兩年研究所生活內對我的照顧，不管是學業上還是生活上，都讓我感到很溫暖。以及在我沒有思緒時提供我一些我想不到的問題切入點，讓我可以用其他種方法來解決同一個問題。以及我的同學雪綸，在得知初稿截止日期時，開始沒日沒夜的趕工，互相鼓勵打氣，直到論文完成，也很開心我們在最後都順利的畢業。

另外我要感謝我的高中同學，韋毅、大誠、文俊、昱辰，以及大誠的大學同學暄雅，在研究所期間彼此互相砥礪，讓我們一起成長，並且在我最低潮失落的時候給我援手，陪我度過難關。

最後，我要感謝我的家人，給予我一個無須擔憂的學習環境，讓我可以好好的在學業上衝刺，如果沒有他們，就不會有今天的劉子堉。

東海大學資訊工程學系 醫學影像實驗室 劉子堉 105 年 7 月

TABLE OF CONTENT

LIST OF TABLES

LIST OF FIGURES

CHAPTER 1

INTRODUCTION

Breast cancer is the abnormal cell growth from breast tissues. The major signs of breast cancer include the change in breast shape, lump in the breast, fluid from the nipple, etc. Breast cancer also be the most common cancer to women in the world. In 2015, about 40290 women and 440 men probably died from breast cancer [1]. Normally, if breast cancer could be detected early, the cure rate would be raised [2]. It is important for early diagnosis that can decrease the mortality effectively.

Mammogram and breast magnetic resonance imaging (MRI) are the most commonly used tools for detecting breast cancer [3]. Mammogram is a good choice, because it is an immediate radiography, noninvasive treatment to patients and inexpensive. Even though mammogram has a plenty of advantages, a great quantity of noises and speckles would not be avoided. However, breast MRI provides high sensitivity to the nidus of breast tissues, multi-view images and non-radiate. However, the disadvantage of MRI is that patients have to bear more economic burden than mammogram.

With the advance of medical imaging technology, computer aided diagnosis (CAD) system is more widespread used in current society [4]. Radiologists also could acquire information that is helpful to them by CAD systems [5], such as the position of the breast or the volume of the breast, even the tumor information, etc. In the past, physicians estimated the volume of the breast by their experience, but it is difficult for physicians with less experience of performing operations. With CAD system, even though physicians and radiologists are inexperienced, they would make a correct

decision immediately [6] [7].

In computer vision, image segmentation is the process to partition a digital image into several segments. The aim of image segmentation is to assist people in acquiring information from images. Image segmentation also is a typical method to locate objects or boundaries in images.

Segmentation methods of breast region could be roughly classified in certain groups: clustering-based [8, 9], region-based [10, 11], edge-based [12, 13], the thresholding method [14] and the hybrid method with over two approaches [15]. Clustering-based method group the pixels that have the same attributes such as K-means clustering method [16]. Region-based approaches divide the image into split parts and connect the homogeneous regions for instance region growing [17]. Edge-based methods used the edge detectors, such as Canny [18] and Sobel [19] methods were performed to border the region of interest (ROI). Thresholding method relied on the change of the grayscale, such as the Otsu's method [20]. This study utilize the hybrid method to detect the breast region. To define the region of the breast, projection techniques are performed to separate the image into the upper region and the lower region and find the start points and the end points of the breast tissue. The upper region is considered to be the breast region, and the lower region is considered to be the inner organ region of body that is definitely to be removed. The task of breast segmentation in this study include two step: segment the upper part of image of the rough pectoral muscle and remove the air area [21].

Wang et al. presented a region based algorithm to detect the pectoral and breast boundary to extract the breast region [22]. Rosado-Toro et al. used K-means++ method to remove the background pixels [23]. Sim et al. introduced a projection method to locate the position of breast area [24]. Jana et al. utilized the edge-enhancement algorithm and the shortest path algorithm to determine the breast region [25].

In order to improve the accuracy of segmentation, image pre-processing plays an important role in whole algorithm. This study perform a pre-processing procedure which utilize the thresholding method, anisotropic filter [26] and morphological close operation to decrease the noise in breast MRI. After this step, the projection method is used to locate the rough pectoral and breast position. At last we compute the pixels of each slice of breast. Further, the volume of the breast would be obtained by accumulating pixels in all slices.

This study present an automated algorithm based on projection to locate the breast to segment the desired ROI. By using projection techniques, the proposed method detect the contour of breast of each slice promptly. By grouping the all slices, the volume of the breast would be estimated. Figure 1.1 shows the flowchart of the proposed method. In the next section, the proposed method and the materials will be described. Section three shows the result of this study. Finally, the conclusion of this study is presented in section four.

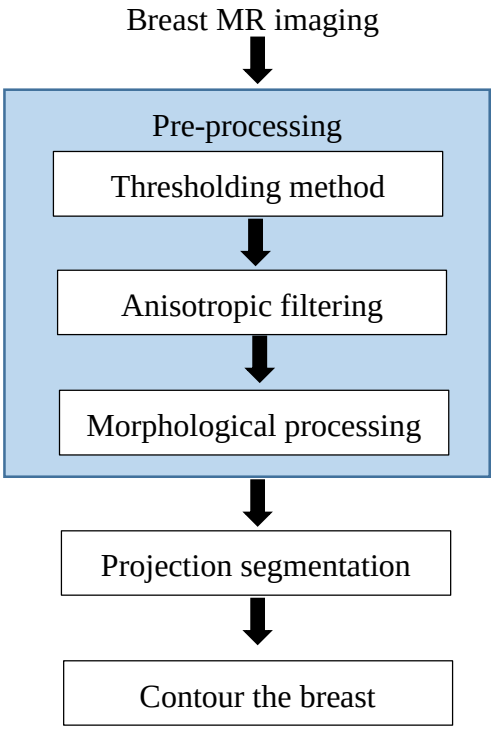

Figure 1.1: Flowchart of the proposed method

CHAPTER 2

MATERIALS AND METHODS

2.1 Data Acquisition

Breast MRI was performed with the patient in the prone position. Examinations were performed with a 3.0-T commercially available system (Verio® ; Siemens AG, Erlangen, Germany) and use of a dedicated16 Channel breast coil. Imaging sequences included a localizing sequence, an axial tse_T1 weighted (3 mm), tse_T2_tirm, pre, during, and post-Gd 3D-FSPGR (1 mm) with fat saturation images, before and five times after rapid bolus injection of 0.1 mmol/L gadobenate dimeglumine (Multihence® ; Bracco, s.p.a., Milano, Italy) per kilogram of body weight at a rate of 2 ml/s; followed by a saline flush, acquired at 60 second intervals were obtained. All obtained images were stored on the hard disk and transferred to a personal computer using a DICOM (Digital Imaging and Communications in Medicine) connection for image analysis.

2.2 Methods

ROI generation is an absolutely necessary step for automatic segmentation in many CAD systems. Most of ROIs are usually irregular shape which provide the rough location of breast area and exclude other tissues as much as possible [27]. In order to get the volume of interest (VOI) of breast, the proposed method detect the ROI and calculated the number of pixels from each image slice. By accumulating the number of pixels per slice, the whole breast volume would be estimated. During detection of ROI in breast MR images, the regions that are insignificant such as lungs, heart and thoracic

cavity must be eliminated cautiously to cut down the computation and promote the accuracy of segmentation [28, 29]. Therefore, a pre-processing procedure is essential in this study. After the pre-processing procedure, the proposed segmentation method utilized projection techniques to locate the breast region. At last, the definition of the lower bound of breast was circumscribed to enhance the precision of segmentation.

2.2.1 Image Pre-processing

Traditional segmentation method would fail with breast MRI because there are a plenty of noises, speckles and tissue textures. Therefore, a pre-processing procedure is necessary for segmentation algorithms. Outstanding pre-processing method make the segmentation go smooth and retain the useful information. In this study, the thresholding method, anisotropic filter and morphological processing were performed as the pre-processing operations.

The first step of the proposed pre-processing method, a thresholding method, is utilized to convert the grayscale images into the binary images that could get rid of the air area in image. The gray-level value of the thresholding method is set as 0.2 to achieve a satisfied result. The value is applicable to the subsequent step.

The second step utilize the anisotropic filter and the morphology processing to treat with the delicate speckles that might influence the result of segmentation. Anisotropic filtering could remove great obstacles and enhance the quality of images, and it could also preserve the boundary information that is important in segmentation phase. Moreover, the morphology processing is applied to adjust the specifics of the image that is operated by anisotropic filter. The closing operation could smooth the edge and fill the hole which is inside of the breast area. The operation provide a positive effect for the proposed segmentation method. Figure 2.1 shows the original image and

the pre-processed result. Figure 2.1(a) is an original MR image which contained abundant information and noises, such as the air area, the breast region and the organs in the body, etc. Figure 2.1(b) shows the image after thresholding method. Figure 2.1(c) shows the image after anisotropic filtering. Figure 2.1(d) shows that the noises were removed in the image.

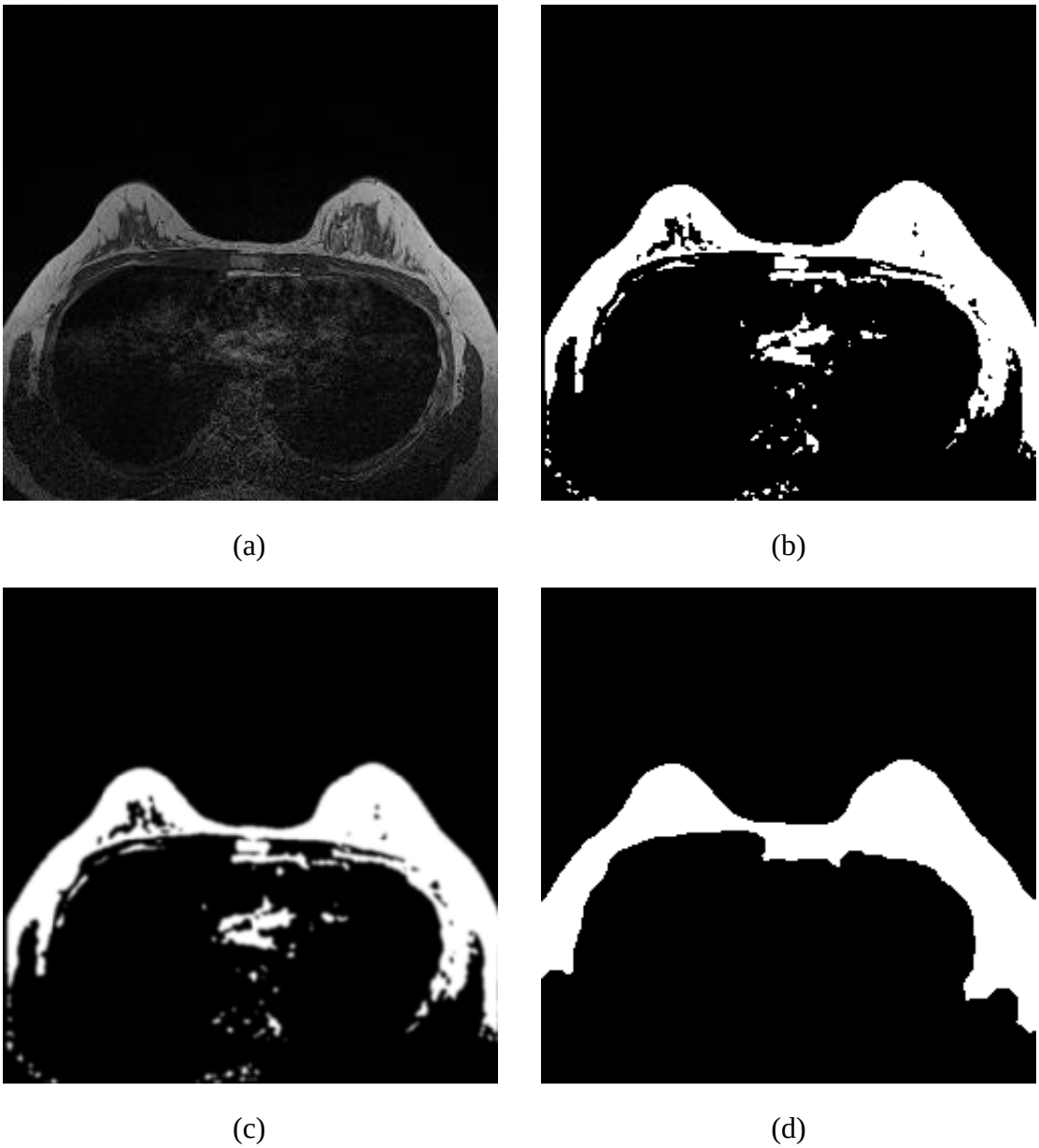

(a) (b)

(c) (d)

Figure 2.1: (a) The original image, (b) After thresholding method, (b) After anisotropic filtering,(d) The pre-processed image

2.2.2 Horizontal Projection Segmentation

The identification of the pectoral position is essential, due to the organs under the pectoral is irrelevant to segment the breast region [24]. Reducing the unnecessary area and making the segmentation go smooth are the purpose for the first step of segmentation. In order to achieve the target, the horizontal projection is performed in this study. The horizontal projection method obtains the histogram that counted by the pixels which value equals to one in the pre-processed image. By this measure, the maximum value could be observed. Thus, the maximum value is set as the point of demarcation. By the coordinate of demarcating point, it is easy to determine the demarcating line to separate the image into the upper region and the lower region.

However, the coordinate of the maximum value might not fit the position of the pectoral. This situation would cause of the segmentation to be fail and to obtain an unexpected result. To avoid the failure condition, the parameter (*h*) is set in the horizontal projection to determine that the demarcating point is in the acceptable range. The determining formula is define as

$$h = \begin{Bmatrix} 250, Hval < 250 \\ 290, Hval \geq 300 \end{Bmatrix}, \tag{2.1}$$

where *Hval* is the coordinate of the maximum value in the whole horizontal projection. Parameter *h* is the modified value for the inapplicable value.

Figure 2.2(a) indicates the coordinate of the maximum value of the image. Consequently, it is simple to separate the image into two parts. The upper part is the interested region in the breast MRI, and on the other, the lower part is insignificant to this study. The green line in Figure 2.2(b) is the border between breast and the internal organs.

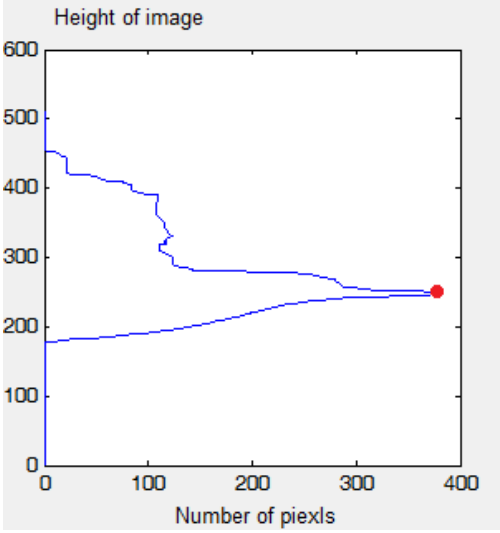

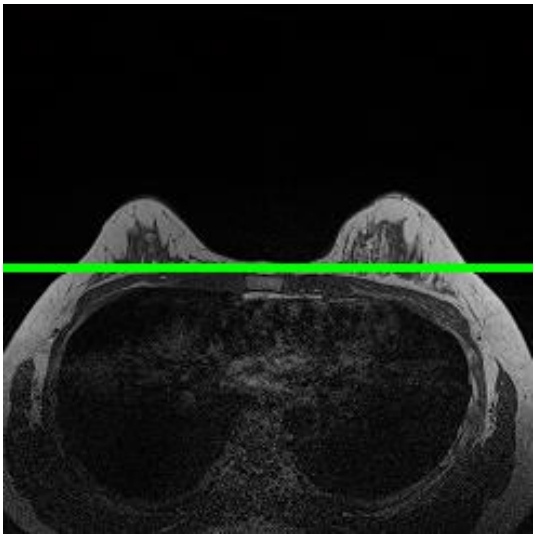

(a) (b)

Figure 2.2: Horizontal projection breast segmentation: (a) Horizontal projection histogram and (b) Segmented breast area.

2.2.3 Vertical Projection Segmentation

The vertical projection is used to separate the breast area and the tissues near the breast. Similar to the horizontal projection, the vertical projection method obtain the histogram that counted by the white pixels in the pre-processed image. Furthermore, the breast region could be segmented more precisely.

The vertical projection is utilized to confirm the range of breast, the histogram curve is similar to that the breast image after pre-processing procedure. Therefore, the definition of the start point and the end point is based on the point that slope begin changing. If the slope is gradually increasing, the first point would be recorded as the start point. On the other hand, if the slope is gradually decreasing, the first point would be recorded as the end point. To prevent the start point and the end point being in the inaccurate position, the parameters *sp* and *ep* were set in the vertical projection to determine that the boundary of the breast is correct or not. The determining formulas are define as

$$sp = \begin{Bmatrix} 320, Svl < \frac{1}{2} ir \;\&\; Svl < Evl \\ Svl \end{Bmatrix} \text{ and} \tag{2.2}$$

$$, ep = \begin{Bmatrix} 200, Evl < \frac{1}{2} ir \;\&\; Evl < Svl \\ Evl \end{Bmatrix}, \tag{2.3}$$

where the parameter *Svl* is the original value of the vertical projection for the start point, *Evl* is the original value of the vertical projection for the end point, respectively. Parameters *sp* and *ep* are the modified values, and the *ir* is the hight of the MRI.

Figure 2.3 demonstrates the result of vertical projection. The start point and the end point are conspicuous. After the start point and the end point identified, the image could be divided in five parts: two outer tissues areas, right breast area, left breast area and the sternum area.

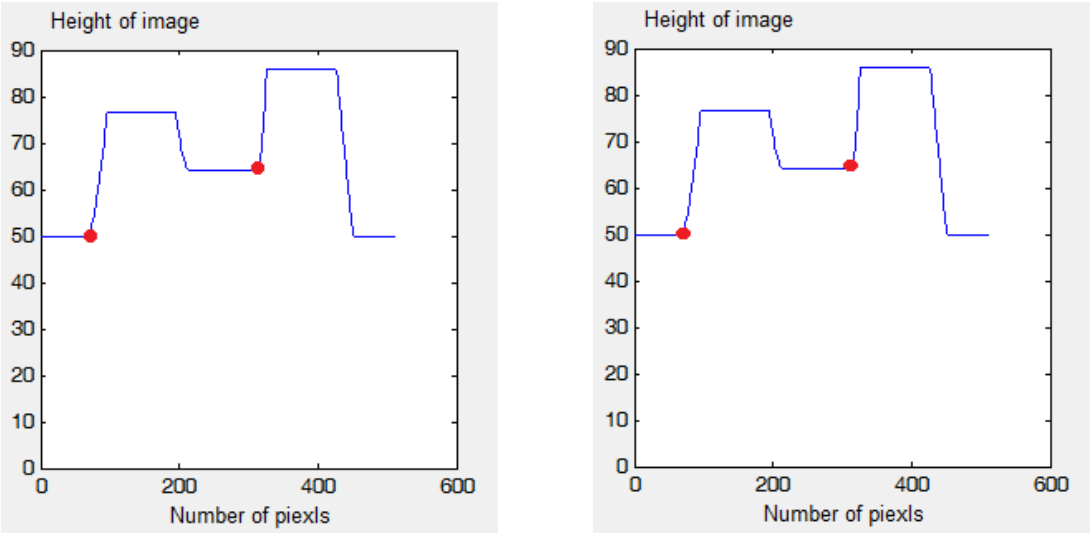

(a) (b)

Figure 2.3: Vertical projection histogram. (a) Coordinates of the start point, (b) Coordinates of the end point.

Figure 2.4(a) displays the segmentation after the vertical projection. The red line is the start point of the breast and the blue line is the end point of the breast. Obviously,

the rough breast boundary was detected. When the horizontal and vertical projection were completed, the breast region could be located. Figure 2.4(b) shows the preliminary result of projection segmentation.

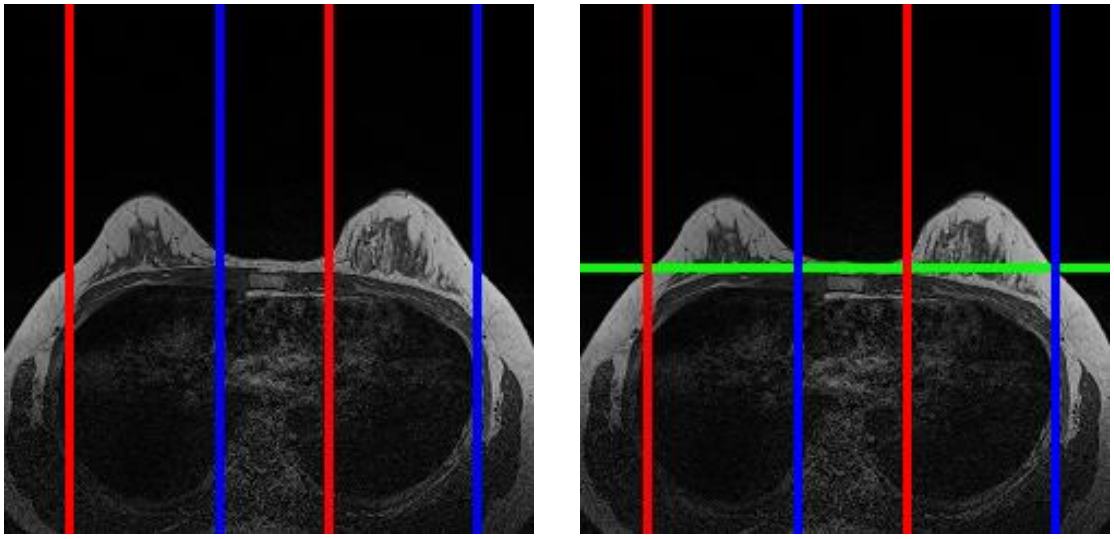

(a) (b)

Figure 2.4: Vertical projection breast segmentation. (a) Segmented breast area, (b) The breast region after horizontal and vertical projection segmentation.

2.2.4 Contouring Breast Region

The preliminary breast region can be found by using the projection method. To optimize the accuracy, the region which is unconcerned with the breast area is supposed to remove. Figure 2.5 demonstrates the result after the horizontal segmentation. The area under the breast is entirely removed. Based on vertical projection segmentation, it is obvious to discriminate breast region from other tissue areas. In general, breast region contains parts of chest tissue which is not relative when physicians operate the breast augmentation surgery.

Due to the highest point in the inner breast and the lowest point in the outer breast,

the lower bound is defined by these two points. The region above the lower bound is the precise breast region. Figure 2.6(a) shows the precise breast region. Figure 2.6(b) shows the all steps required to generate the result of the automatic segmentation in the original breast MRI.

Figure 2.5: The result after the horizontal segmentation.

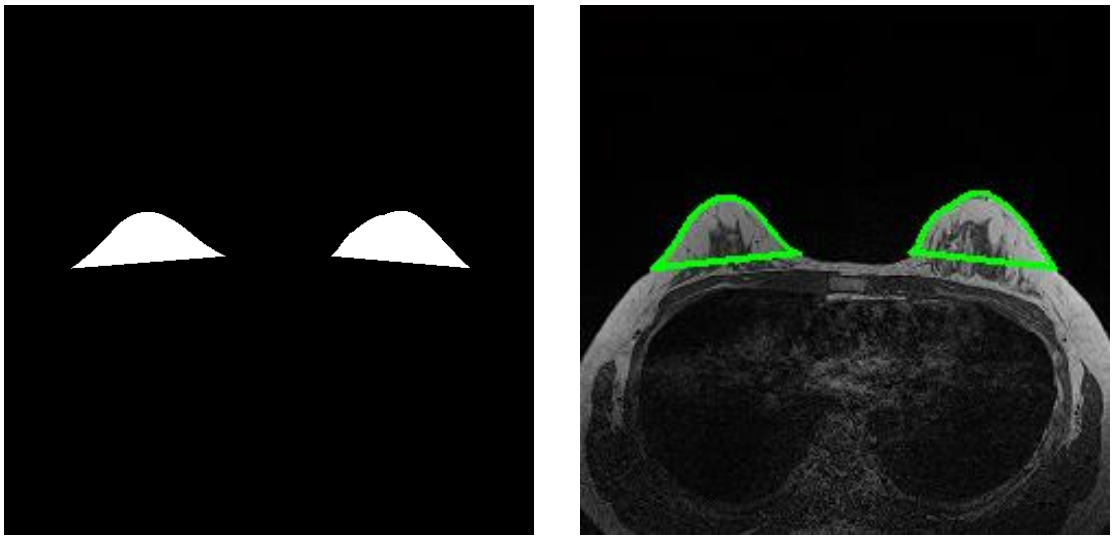

(a) (b)

Figure 2.6: The result of the automatic segmentation. (a) Precise breast region, (b) The result of the automatic segmentation in the original MR image.

CHAPTER 3

Simulation Results

3.1 Dataset

The experiment of the proposed method was implemented by using axial breast MR images dataset (12 cases). The images were accumulated by comprehensive Breast Cancer Center of Changhua Christian Hospital at Changhua in Taiwan.

In the aggregate, 12 sets of MR breast images are used. The resolution of the nine sets is 512 × 512 × 60 with 16 bits per pixel, the resolution of other two sets is 512 × 512 × 45 with 16 bits per pixel. the resolution of the last one set is 448 × 448 × 60 with 16 bits per pixel. Field of view (FOV) of the images is 320 mm and the slice thickness is 3 mm. The proposed automatic segmentation method was implemented by Matlab (R2012a, MathWorks Inc., MA). The simulations were performed on a Windows PC with i7 (3.6 GHz) processor and 8GB memory. The boundary of the breast was manually sketched by experienced radiologists. The performance of the proposed algorithm was proved by comparing with the result of the radiologists' breast contour.

3.2 Evaluation of Contour

The four practical similarity measures, the similarity index (*SI*), overlap fraction (*OF*), over value (*OV*), and extra fraction (*EF*), between the manually sketched contours and the automatically determined contours are calculated for the quantitative analysis [30]. REF stands for the results delineated by the physician manually, and SEG represents the region of breast depicted by our automatic segmentation method. *SI* is

the similar degree between REF and SEG. The overlap area comprises the area of the proposed method and manual sketching by physician, extra area means the false positive area and missing area means false negatives area. The four similarity measures are defined as

$$SI = \frac{2 * (REF \bigcap SEG)}{REF + SEG}, \tag{3.1}$$

$$OF = \frac{REF \bigcap SEG}{REF}, \tag{3.2}$$

$$OV = \frac{REF \bigcap SEG}{REF \bigcup SEG}, \tag{3.3}$$

$$\text{and} \quad EF = \frac{\overline{REF} \bigcap SEG}{REF}. \tag{3.4}$$

When *SI*, *OF*, *OV* are close to 1, and *EF* is close to 0, it indicates that the breast area segmented by our method is similar to the result that sketched by physician.

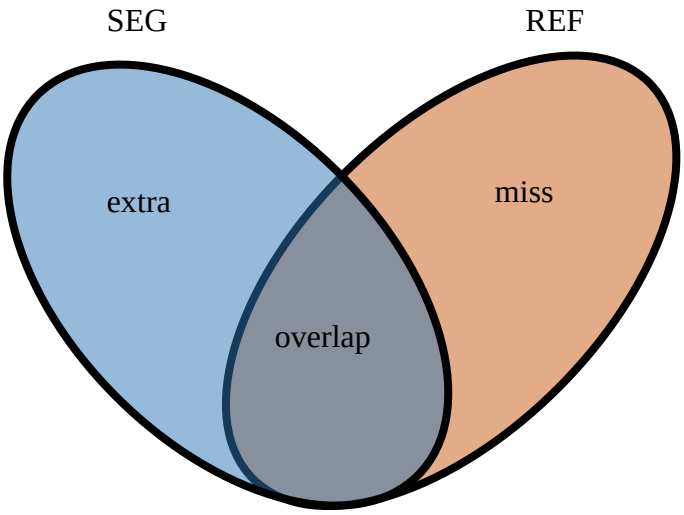

Figure 3.1: The relationship between breast region segmentation by SEG (segmented by our method) and REF (manually sketched by physician).

3.3 Segmentation Results

For presenting the segmentation method 12 cases are considered. In the all case, the demarcating line is set to divide the MRI image into the upper part and the lower part. The lower part of MRI image is removed immediately since it is the position of the inner organs. By the start point and the end point, the breast tissues are restricted. In order to increase the identifiability of image, the insignificant area in the MRI image should be removed. The segmentation result of proposed method are shown on Figure (3.2-3.13). Figures 3.2(a) to 3.13(a) show the original breast MRI. Figures 3.2(b) to 3.13(b) show the contours determined by our system. Figures 3.2(c) to 3.13(c) show the region which sketched manually by physician. In Figs. (3.14-3.25), the contour presented by our system were overlapped with the contour delineated by radiologist. Clearly, the breast region determined by the proposed system is similar to the sketching by physician indeed. Performance analysis was evaluated through the four practical similarity measures.

Table 3.1 shows the value of *SI*, *OF*, *OV*, *EF* for each case. The average measures (*SI*, *OF*, *OV*, *EF*) of proposed method are (0.94, 0.92, 0.88, 0.11). The highest value of (*SI*, *OF*, *OV*) could reach (0.95, 0.95, 0.91), and the lowest value of (*EF)* is (0.08) that mean the segmentation result is similar to the delineation sketched by physician.

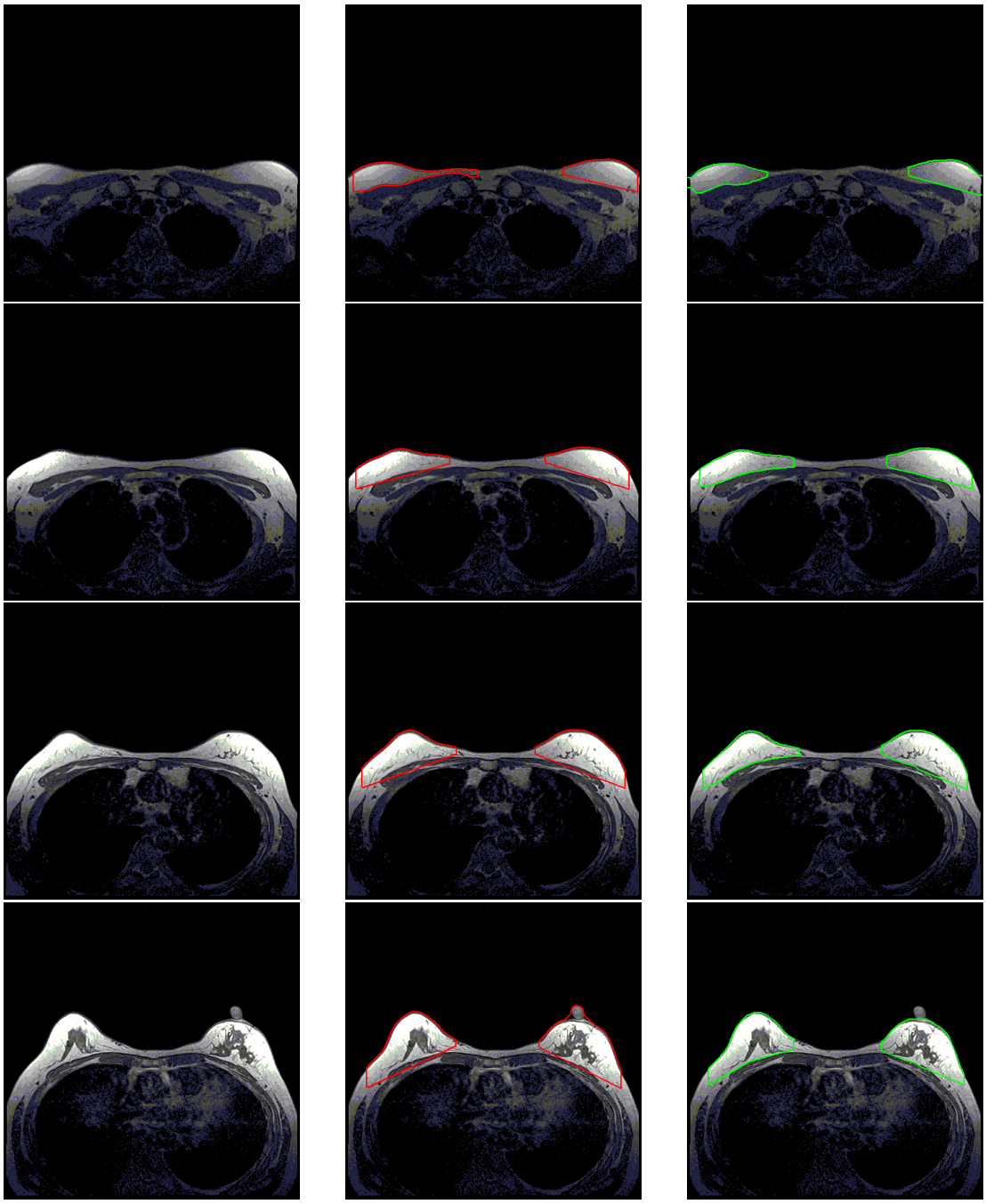

(a) (b) (c)

Figure 3.2: The result of case 1 of proposed method (60 slices per case). (a) The original DICOM images, (b) segmented result, (c) manually sketched result. (Continued)

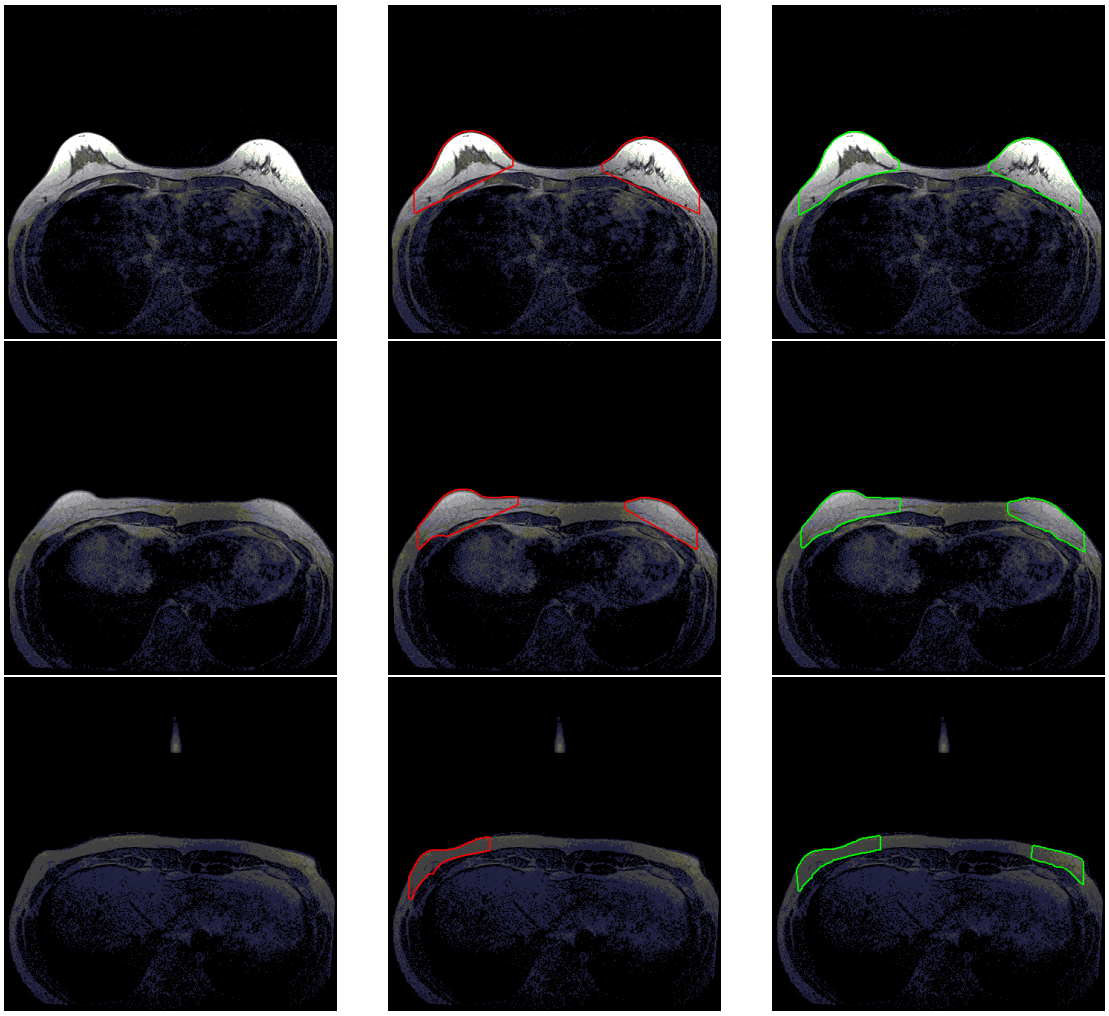

(a) (b) (c)

Figure 3.2: The result of case 1 of proposed method (60 slices per case). (a) The original DICOM images, (b) segmented result, (c) manually sketched result.

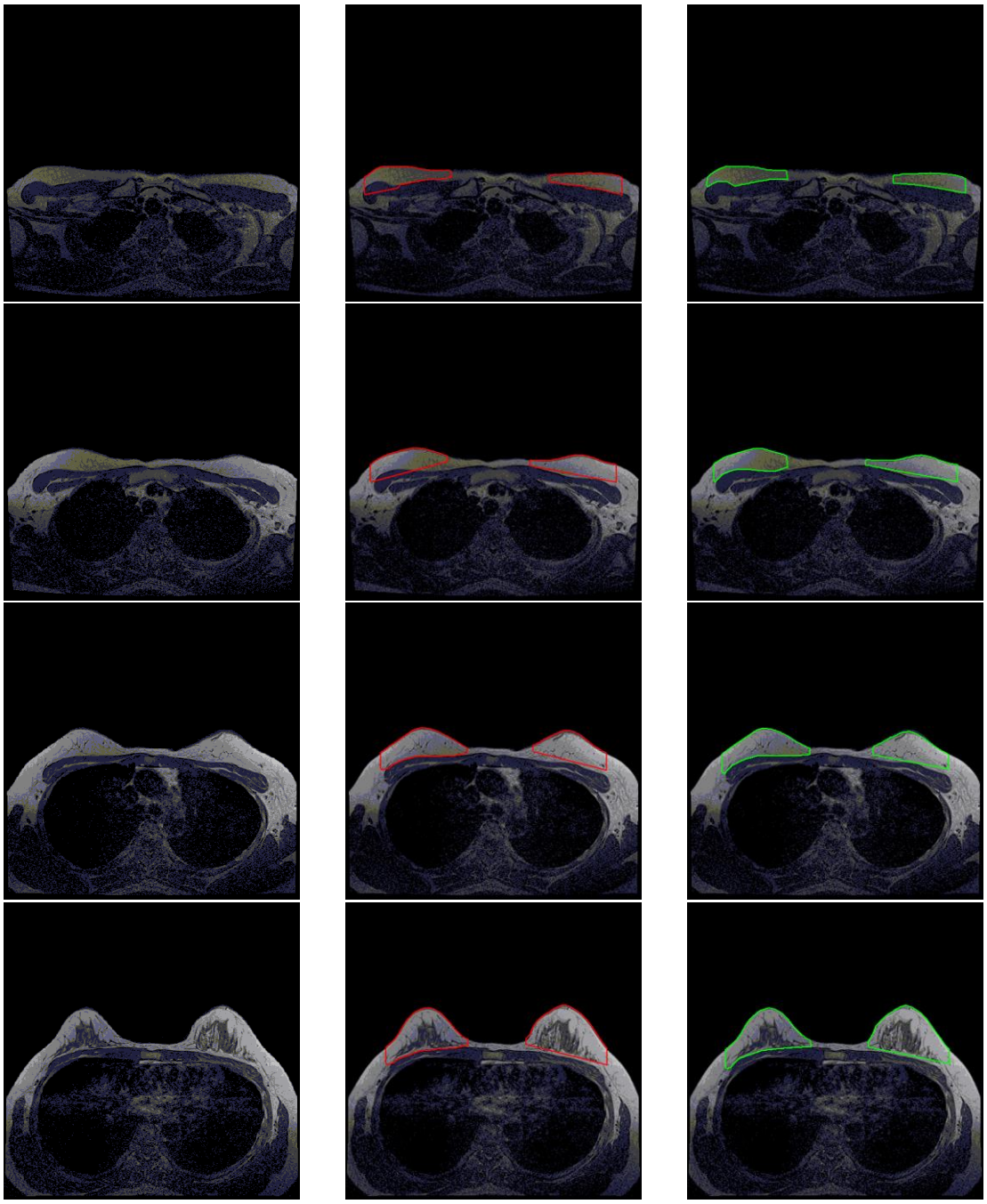

(a) (b) (c)

Figure 3.3: The result of case 2 of proposed method (60 slices per case). (a) The original DICOM images, (b) segmented result, (c) manually sketched result. (Continued)

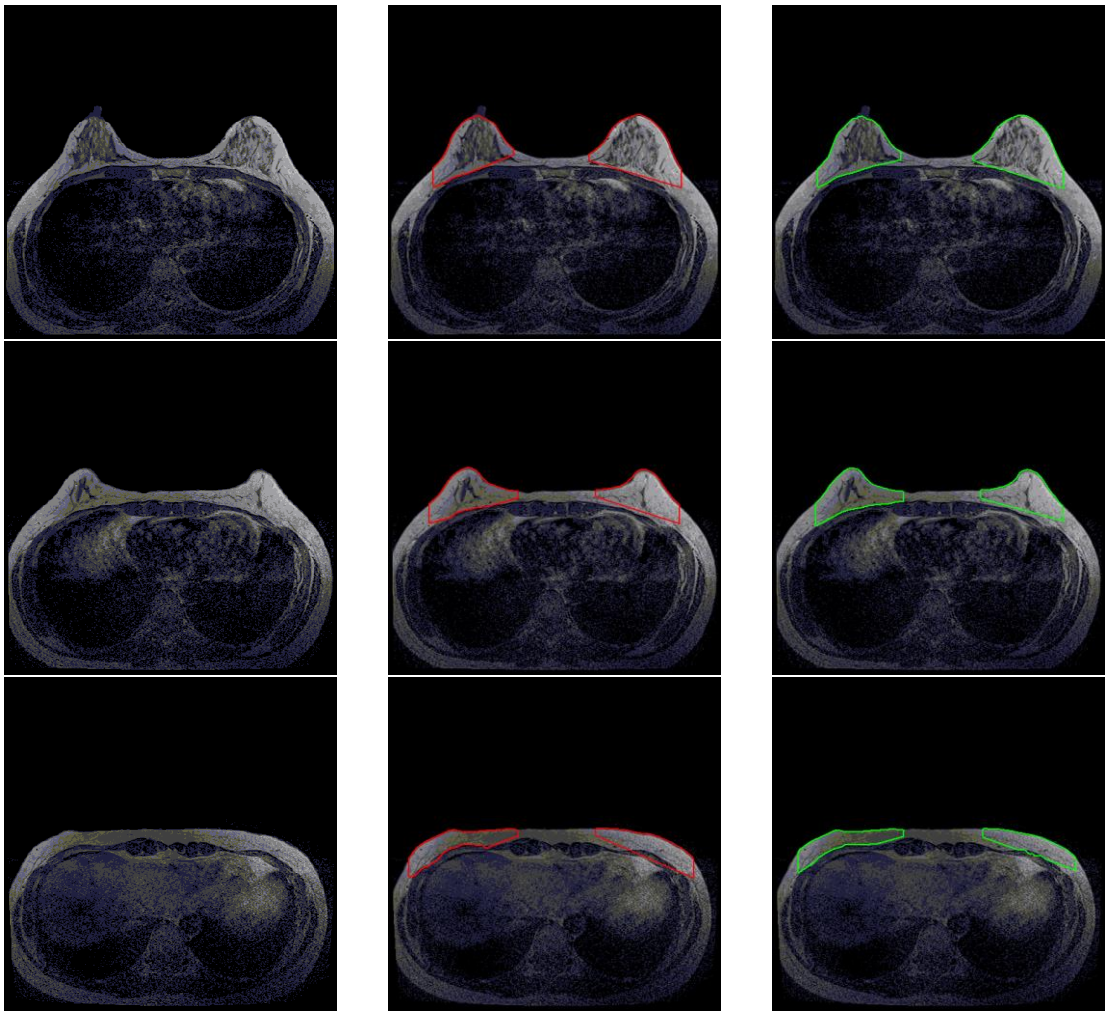

(a) (b) (c)

Figure 3.3: The result of case 2 of proposed method (60 slices per case). (a) The original DICOM images, (b) segmented result, (c) manually sketched result.

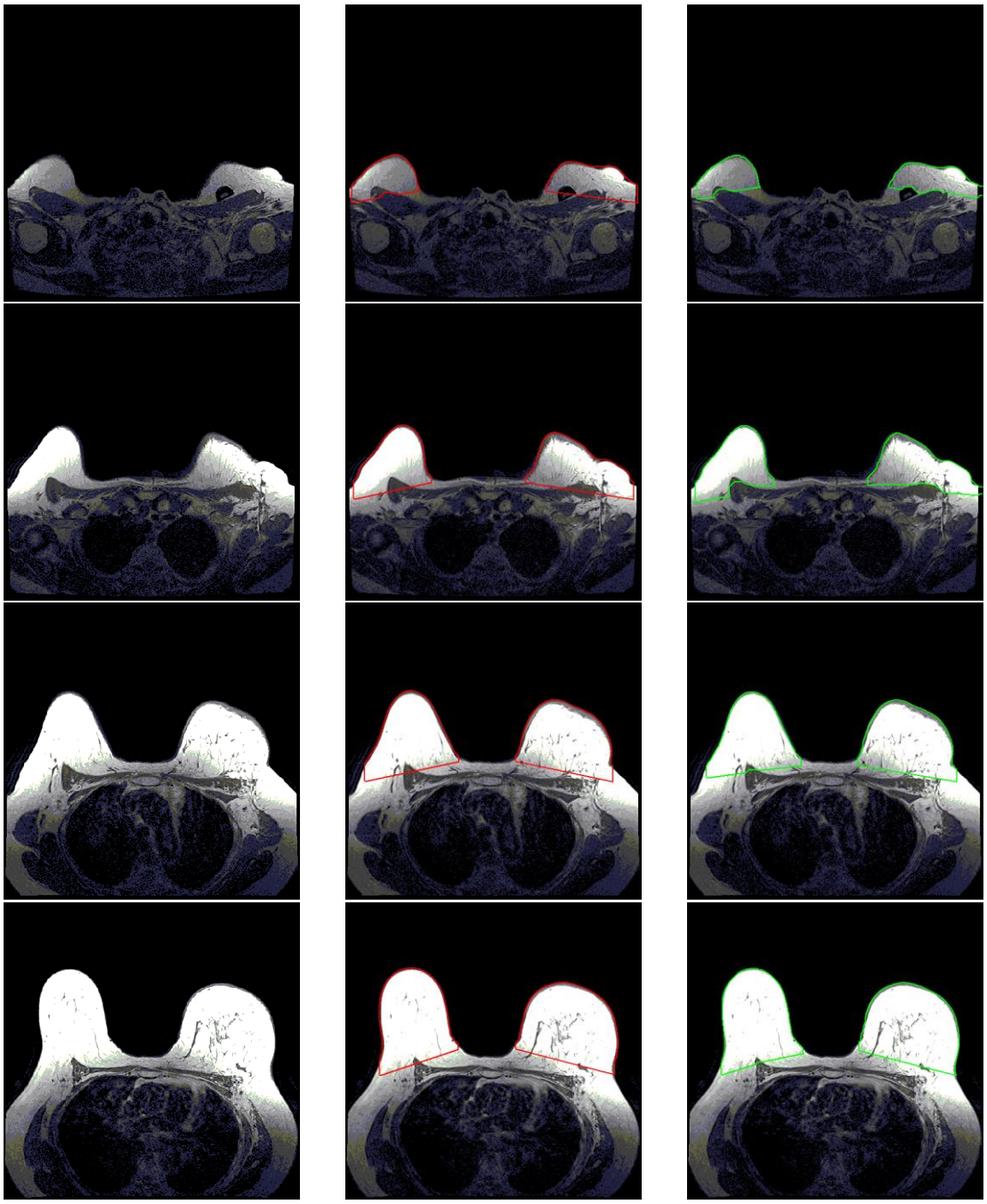

(a) (b) (c)

Figure 3.4: The result of case 3 of proposed method (60 slices per case). (a) The original DICOM images, (b) segmented result, (c) manually sketched result. (Continued)

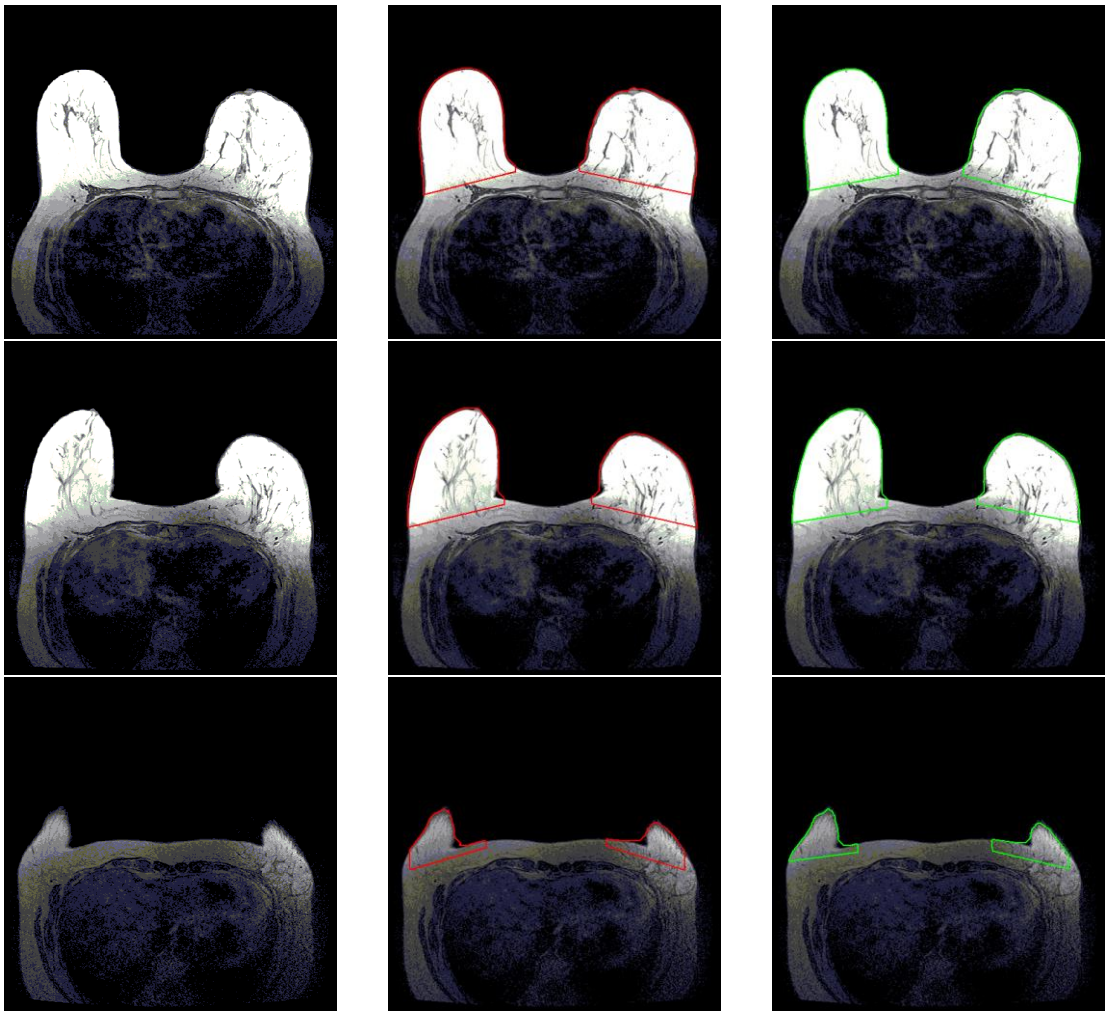

(a) (b) (c)

Figure 3.4: The result of case 3 of proposed method (60 slices per case). (a) The original DICOM images, (b) segmented result, (c) manually sketched result.

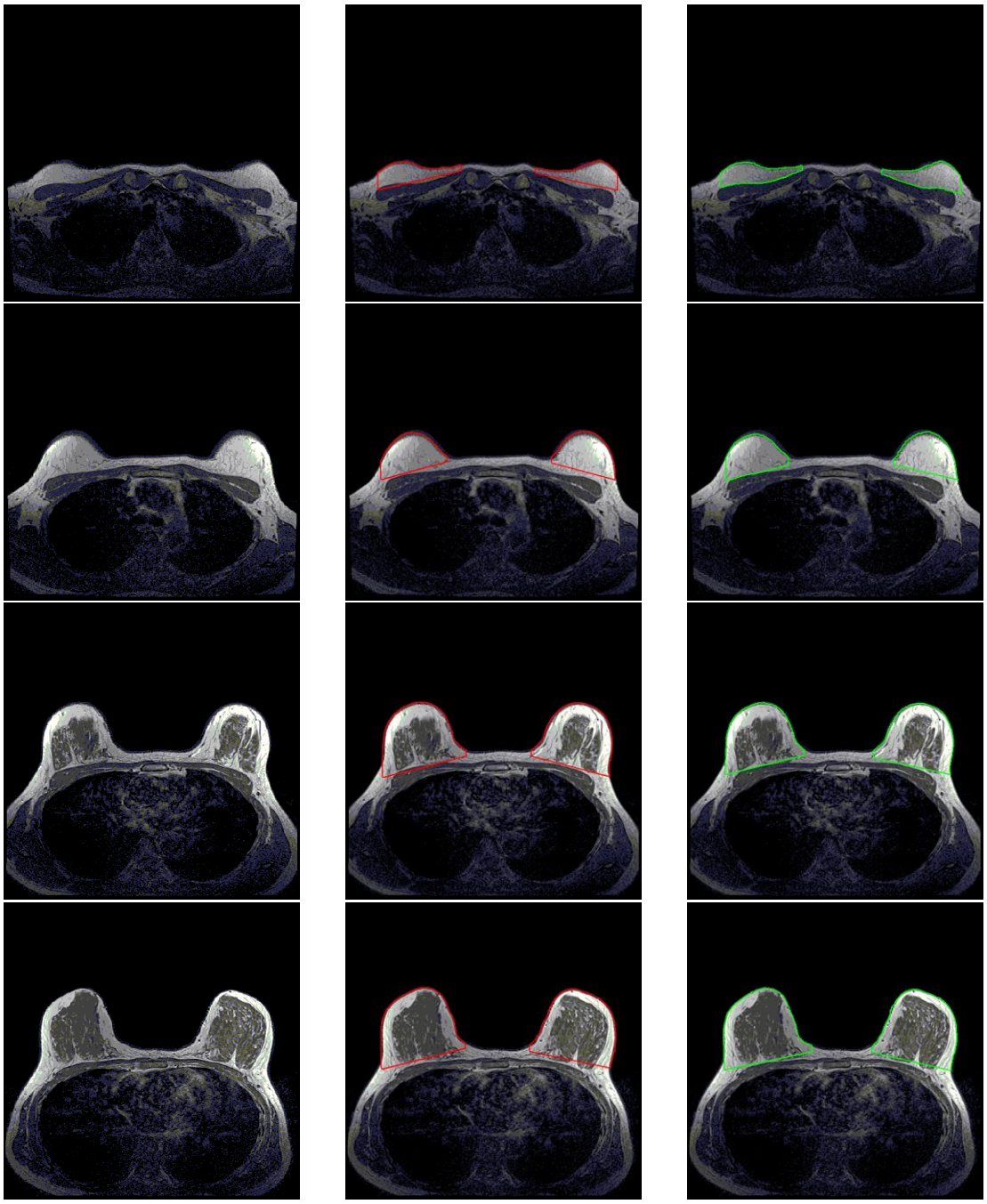

(a) (b) (c)

Figure 3.5: The result of case 4 of proposed method (60 slices per case). (a) The original DICOM images, (b) segmented result, (c) manually sketched result. (Continued)

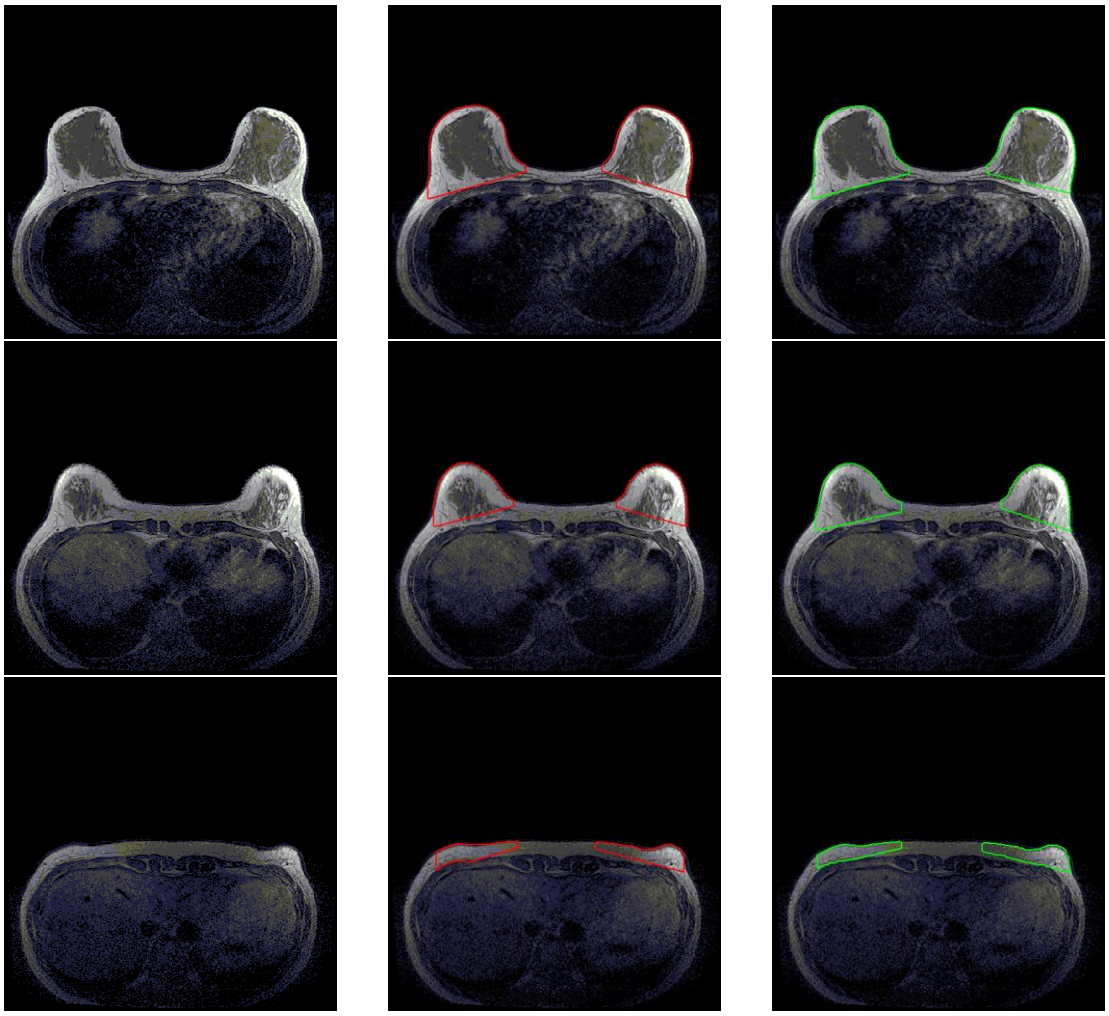

(a) (b) (c)

Figure 3.5: The result of case 4 of proposed method (60 slices per case). (a) The original DICOM images, (b) segmented result, (c) manually sketched result.

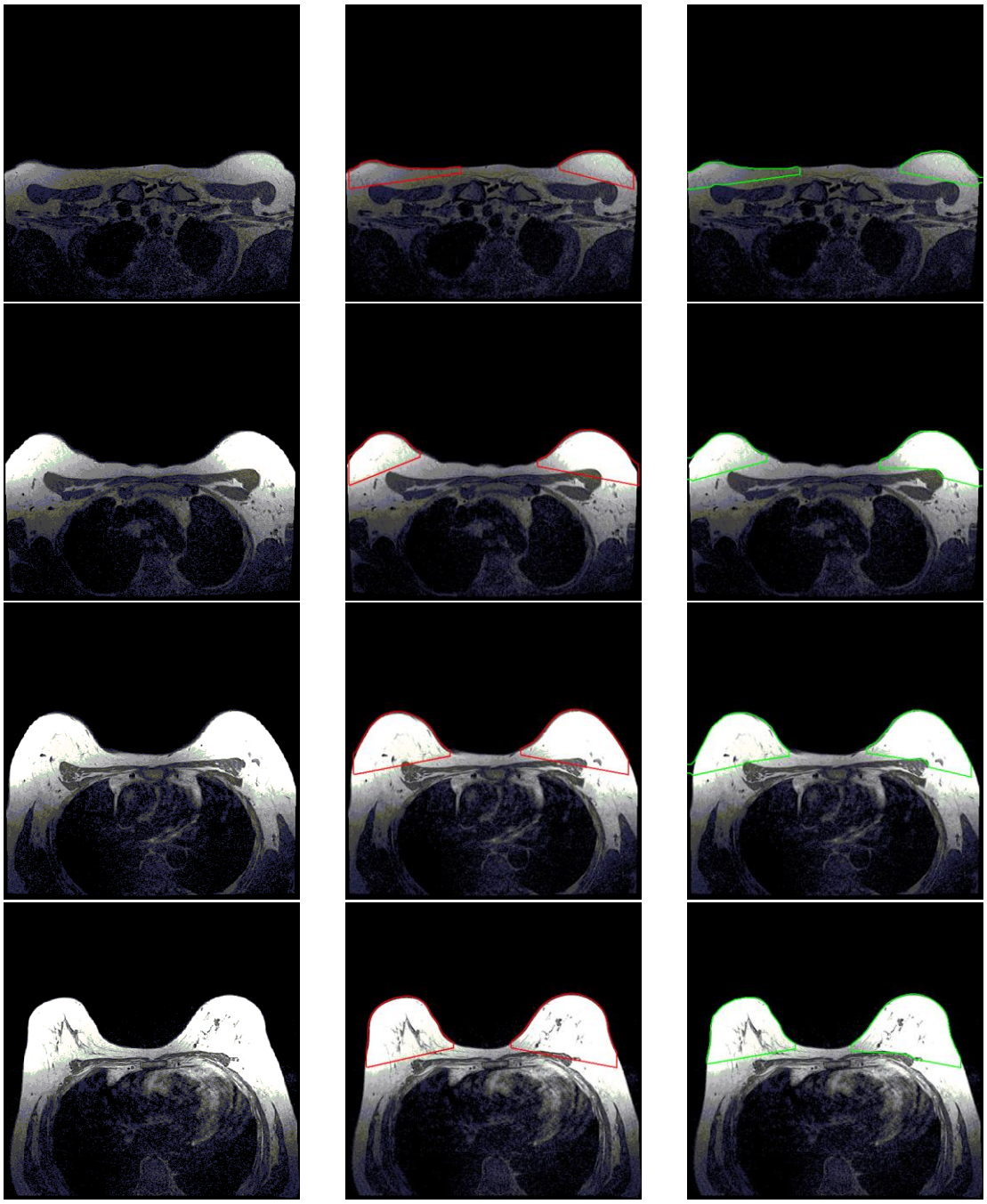

(a) (b) (c)

Figure 3.6: The result of case 5 of proposed method (60 slices per case). (a) The original DICOM images, (b) segmented result, (c) manually sketched result. (Continued)

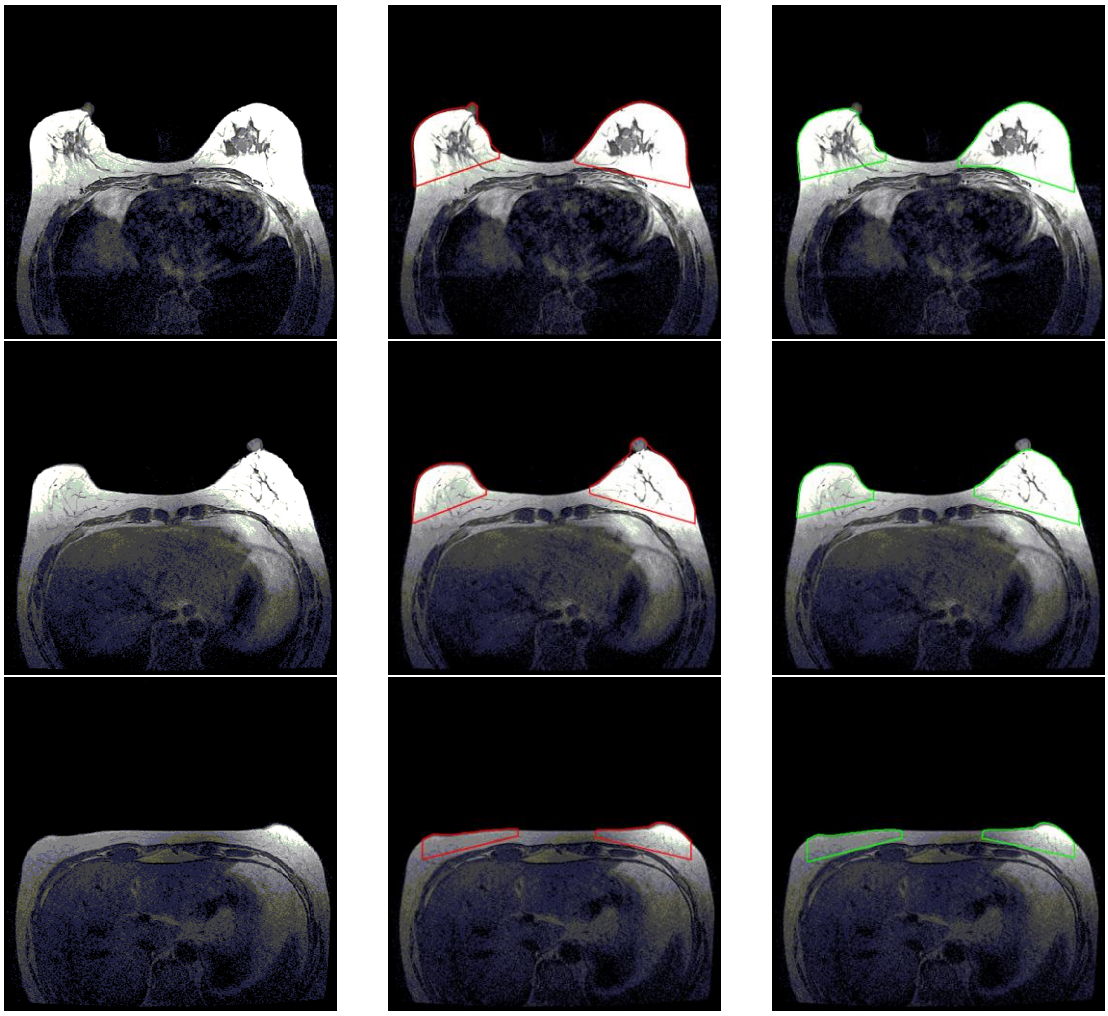

(a) (b) (c)

Figure 3.6: The result of case 5 of proposed method (60 slices per case). (a) The original DICOM images, (b) segmented result, (c) manually sketched result.

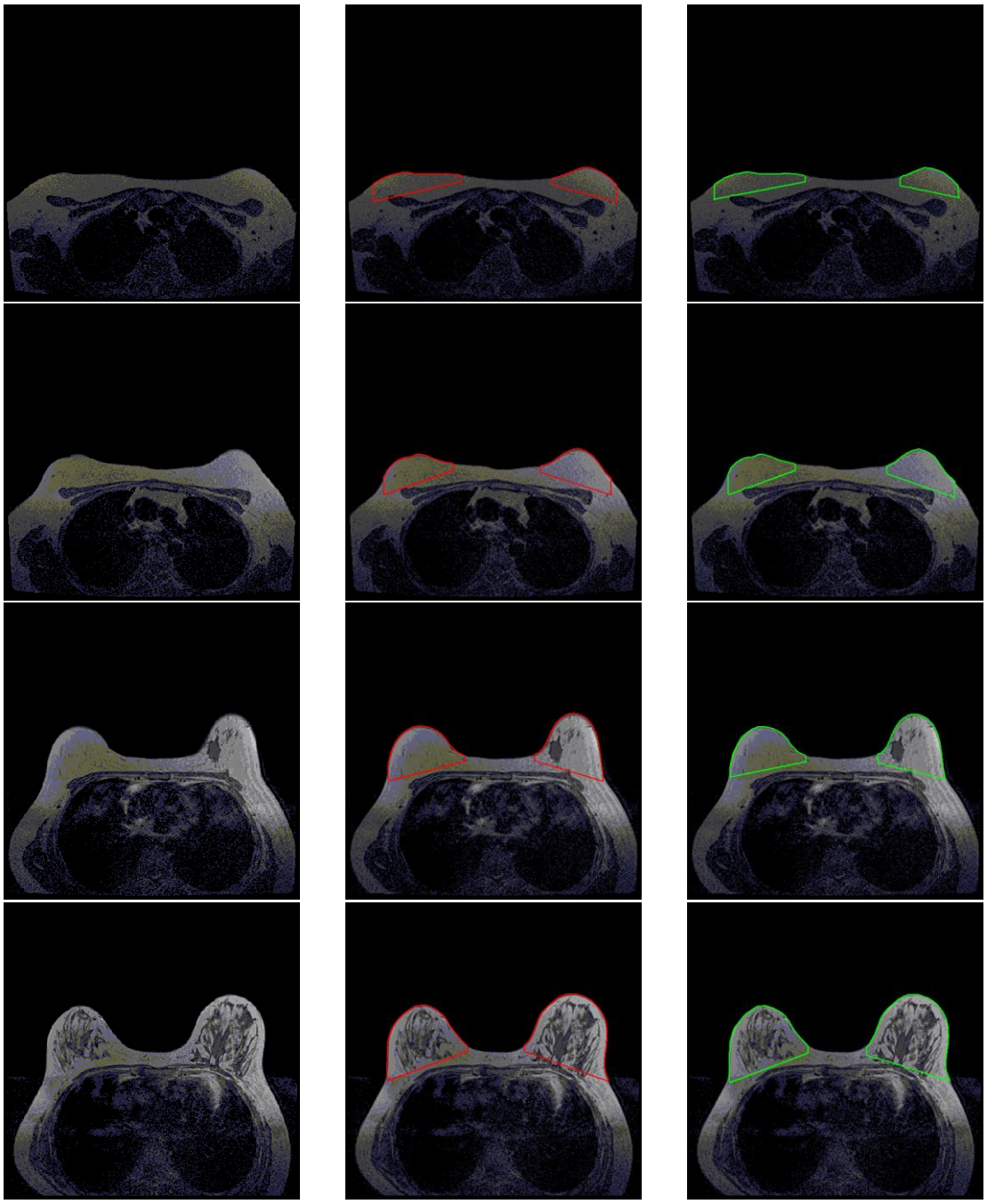

(a) (b) (c)

Figure 3.7: The result of case 6 of proposed method (60 slices per case). (a) The original DICOM images, (b) segmented result, (c) manually sketched result. (Continued)

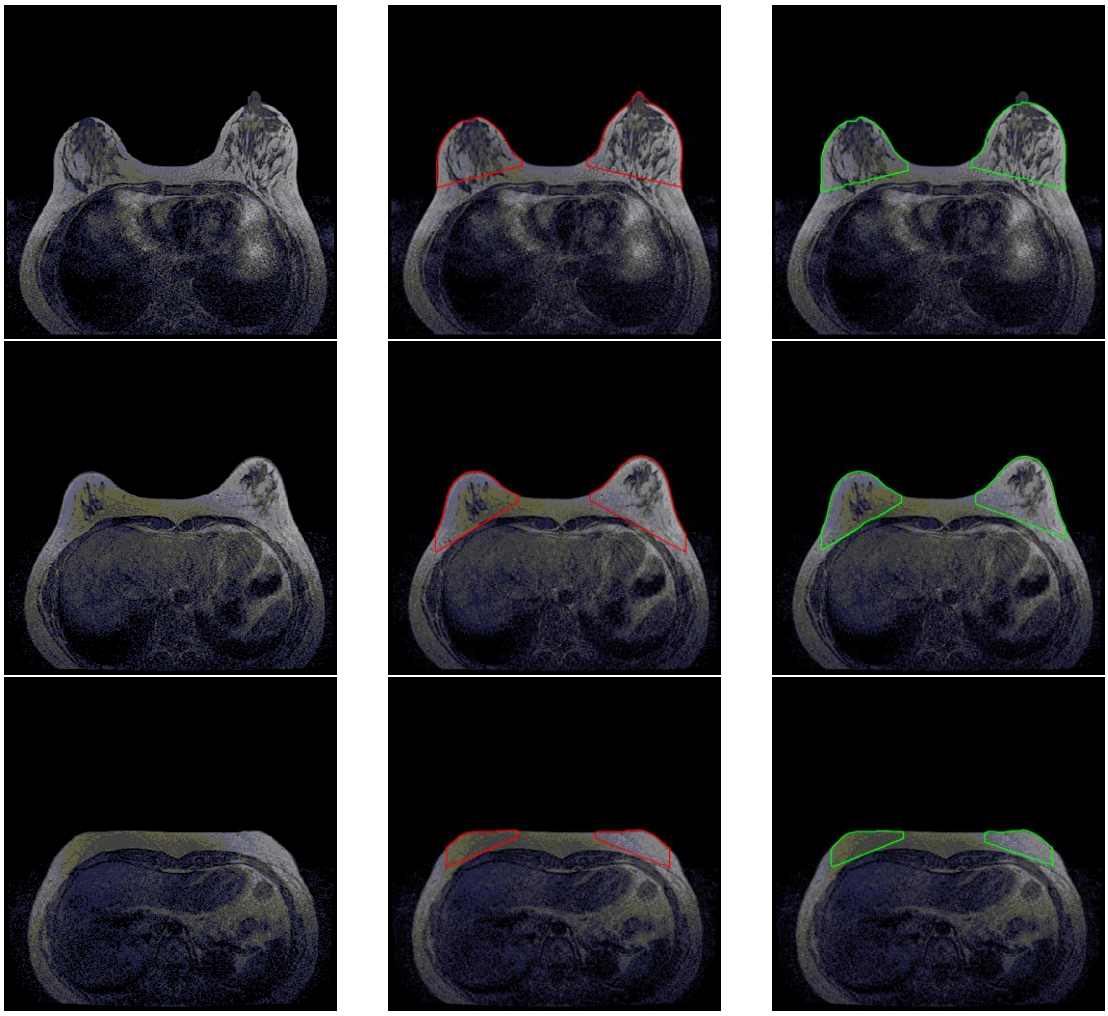

(a) (b) (c)

Figure 3.7: The result of case 6 of proposed method (60 slices per case). (a) The original DICOM images, (b) segmented result, (c) manually sketched result.

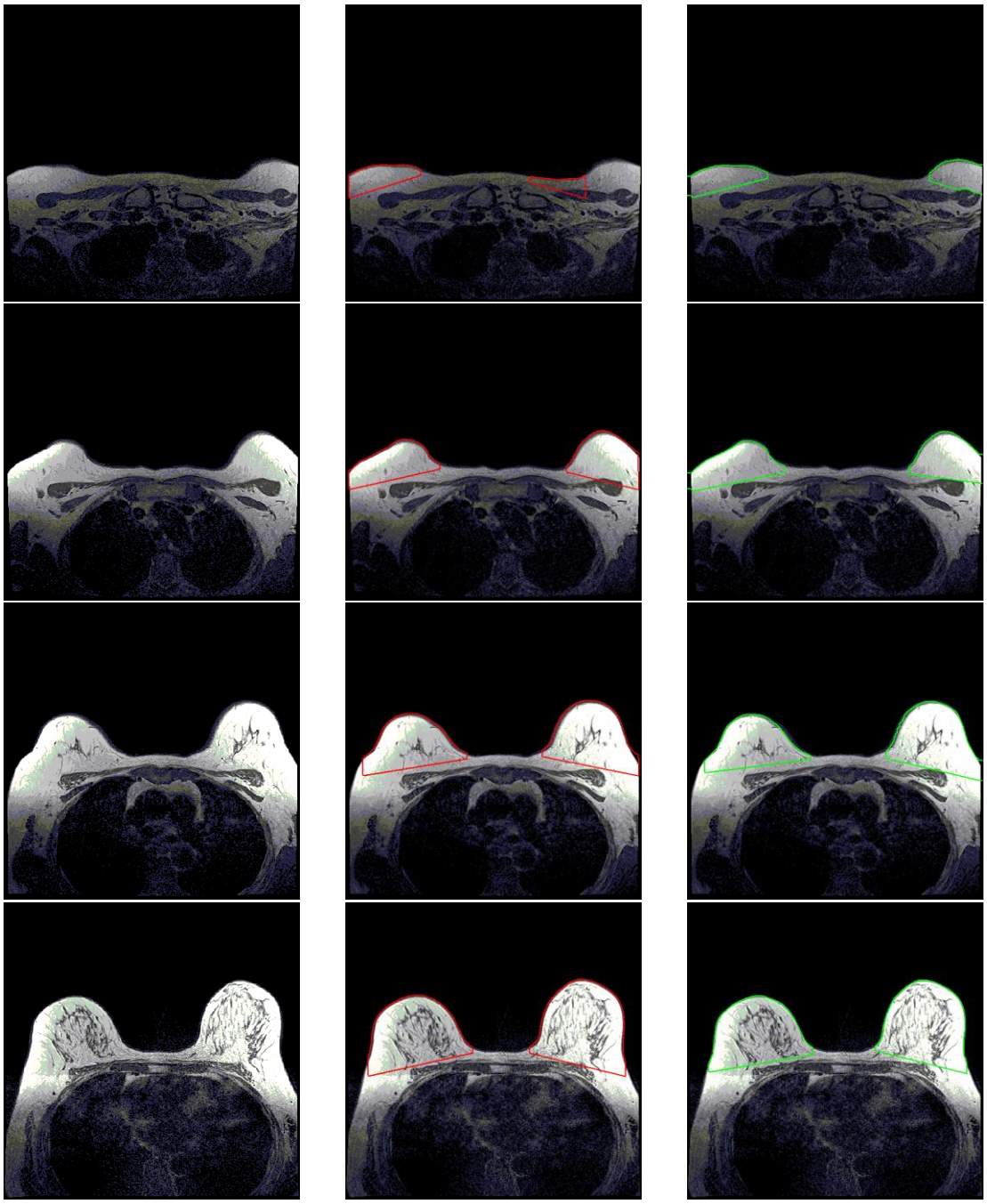

(a) (b) (c)

Figure 3.8: The result of case 7 of proposed method (60 slices per case). (a) The original DICOM images, (b) segmented result, (c) manually sketched result. (Continued)

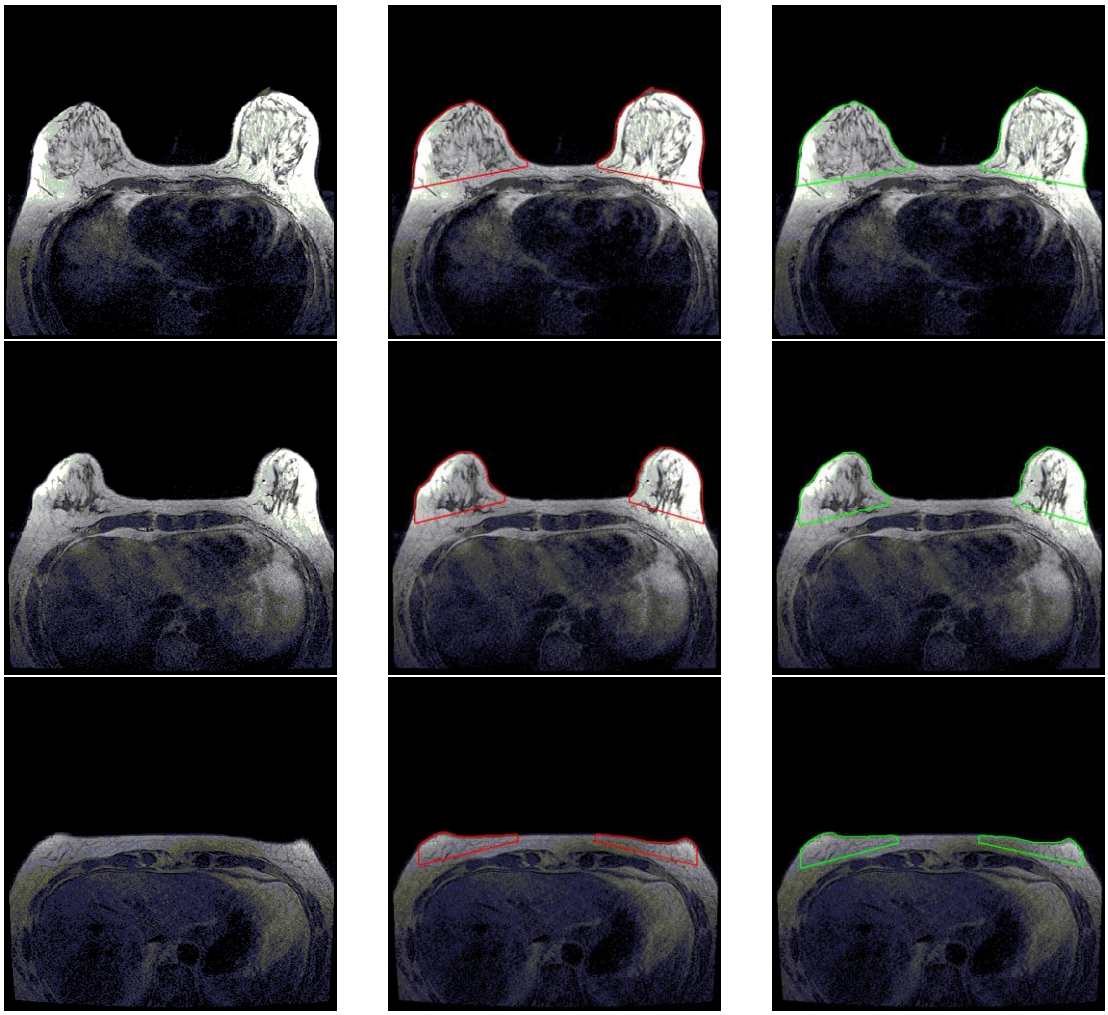

(a) (b) (c)

Figure 3.8: The result of case 7 of proposed method (60 slices per case). (a) The original DICOM images, (b) segmented result, (c) manually sketched result.

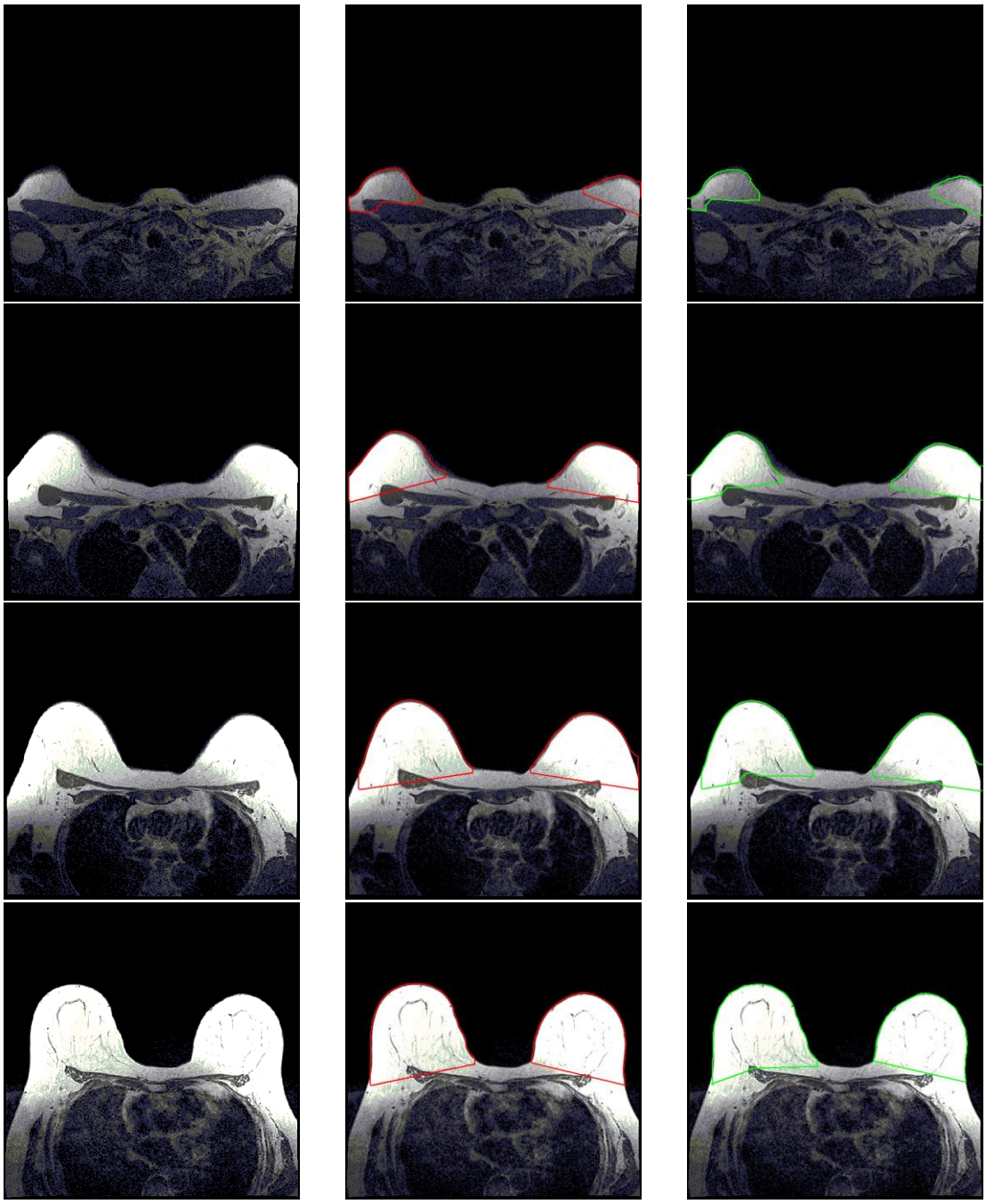

(a) (b) (c)

Figure 3.9: The result of case 8 of proposed method (60 slices per case). (a) The original DICOM images, (b) segmented result, (c) manually sketched result. (Continued)

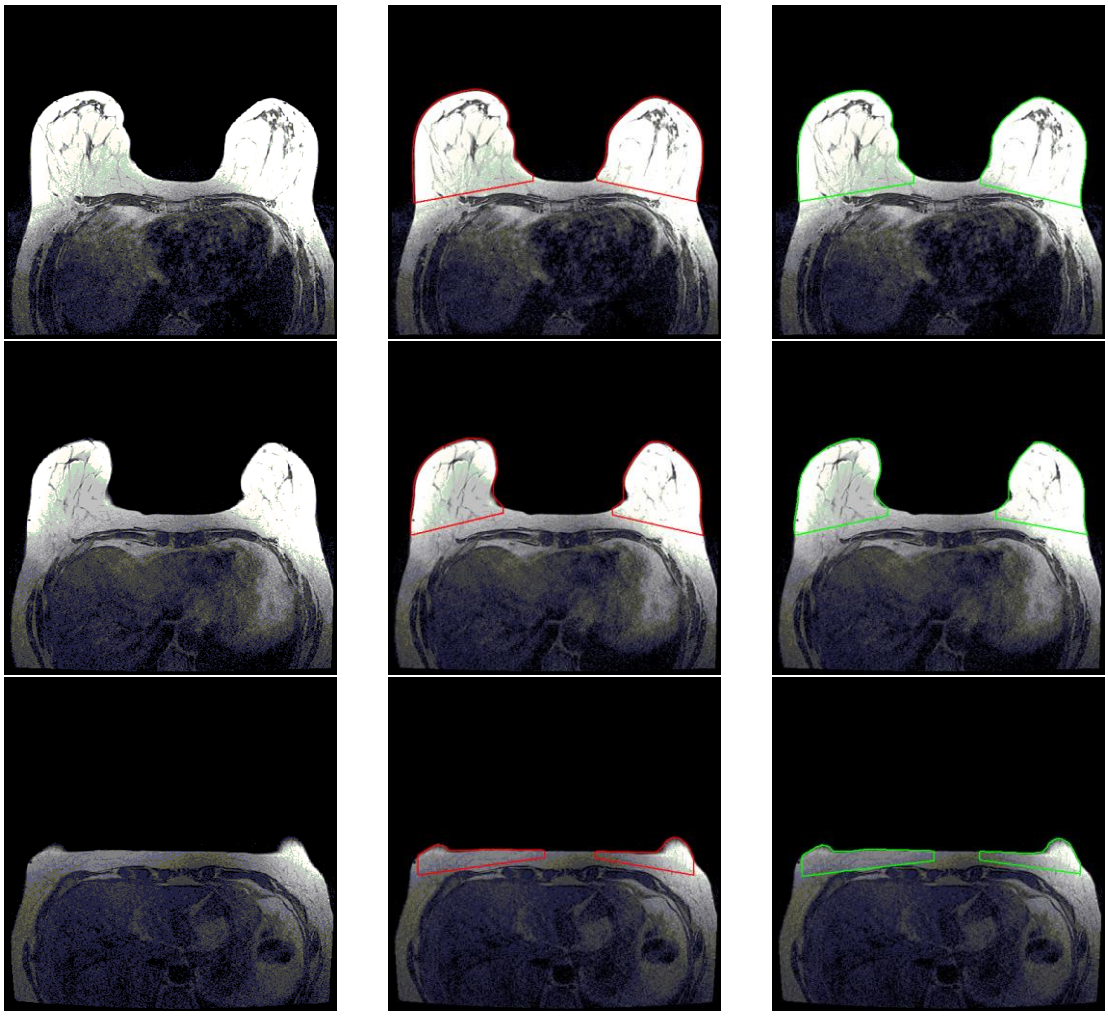

(a) (b) (c)

Figure 3.9: The result of case 8 of proposed method (60 slices per case). (a) The original DICOM images, (b) segmented result, (c) manually sketched result.

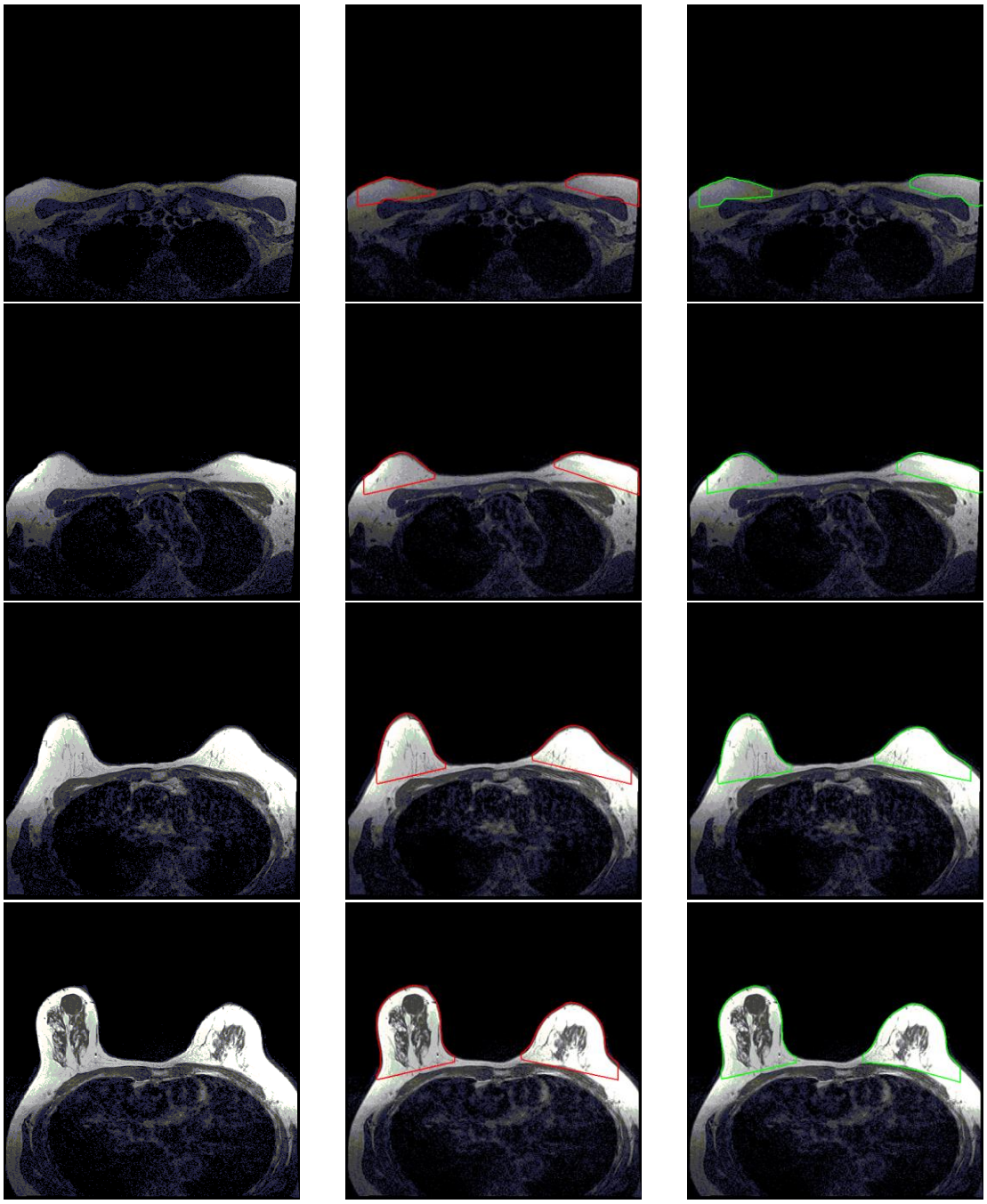

(a) (b) (c)

Figure 3.10: The result of case 9 of proposed method (60 slices per case). (a) The original DICOM images, (b) segmented result, (c) manually sketched result. (Continued)

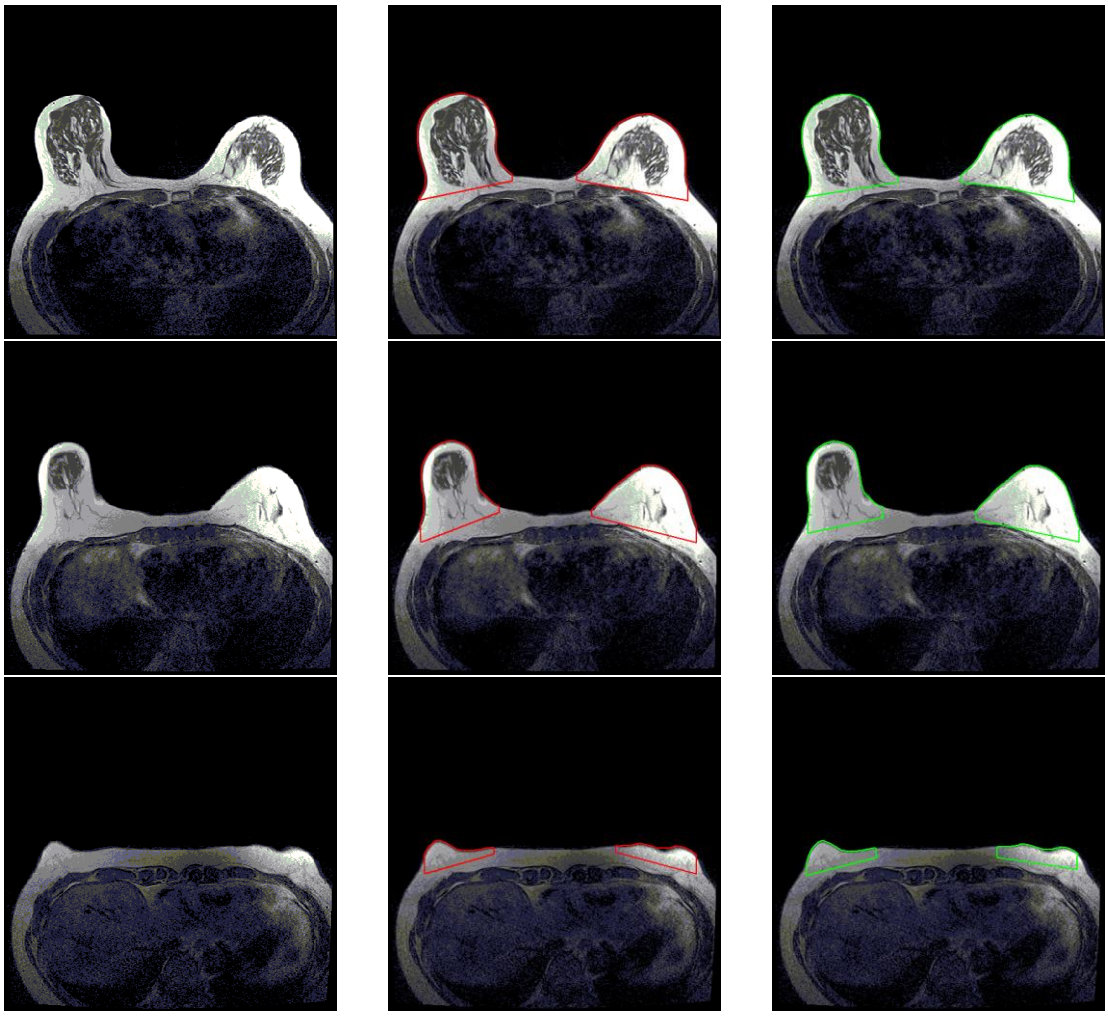

(a) (b) (c)

Figure 3.10: The result of case 9 of proposed method (60 slices per case). (a) The original DICOM images, (b) segmented result, (c) manually sketched result.

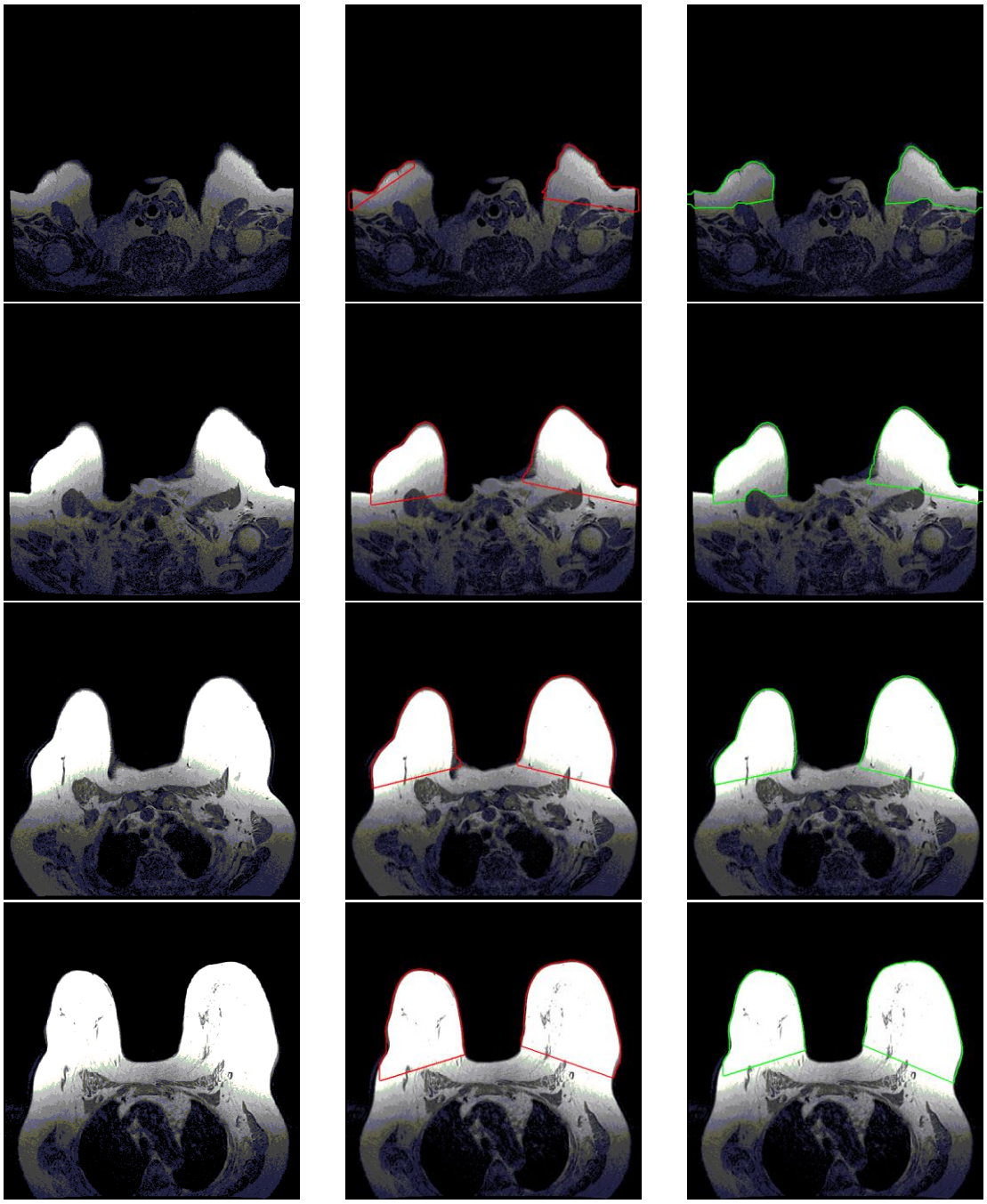

(a) (b) (c)

Figure 3.11: The result of case 10 of proposed method (60 slices per case). (a) The original DICOM images, (b) segmented result, (c) manually sketched result. (Continued)

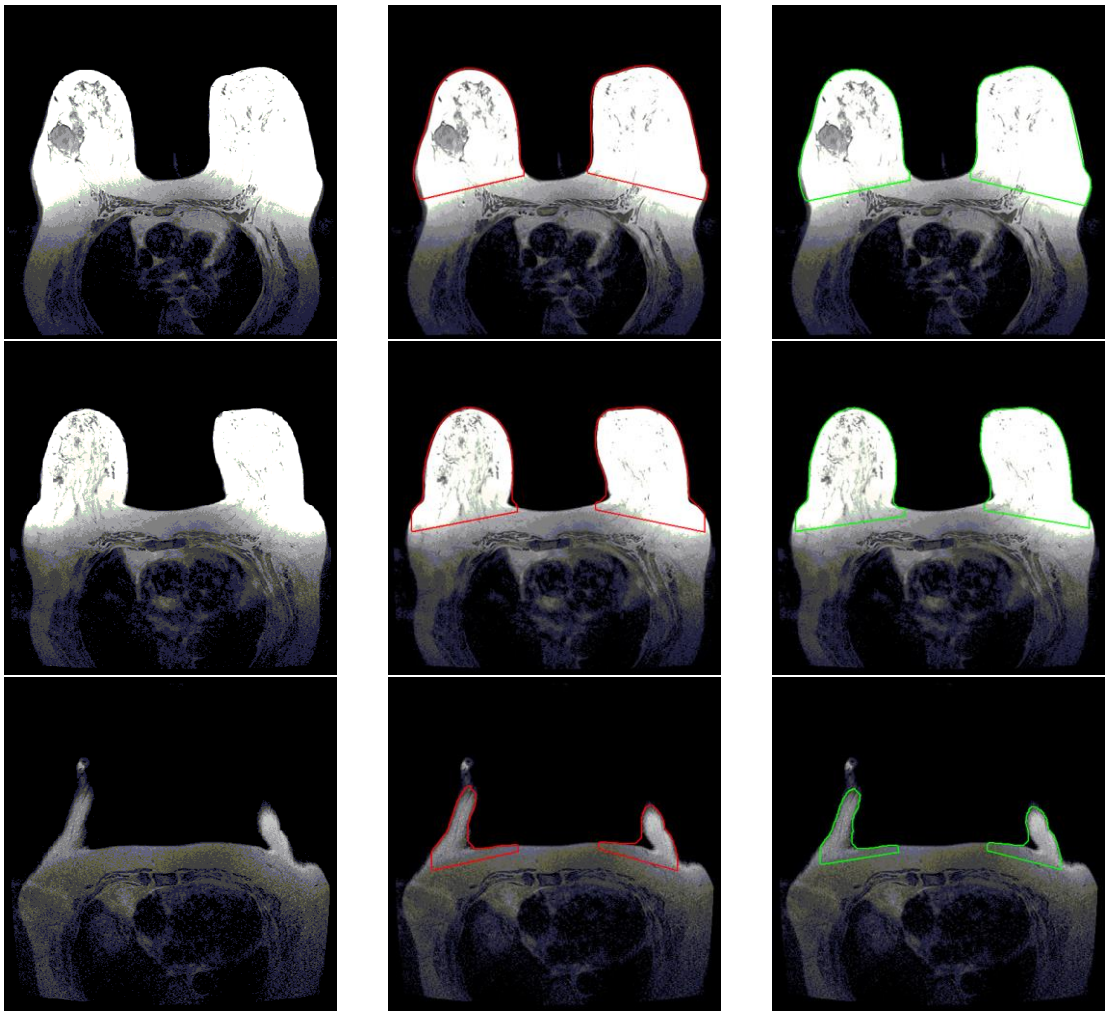

(a) (b) (c)

Figure 3.11: The result of case 10 of proposed method (60 slices per case). (a) The original DICOM images, (b) segmented result, (c) manually sketched result.

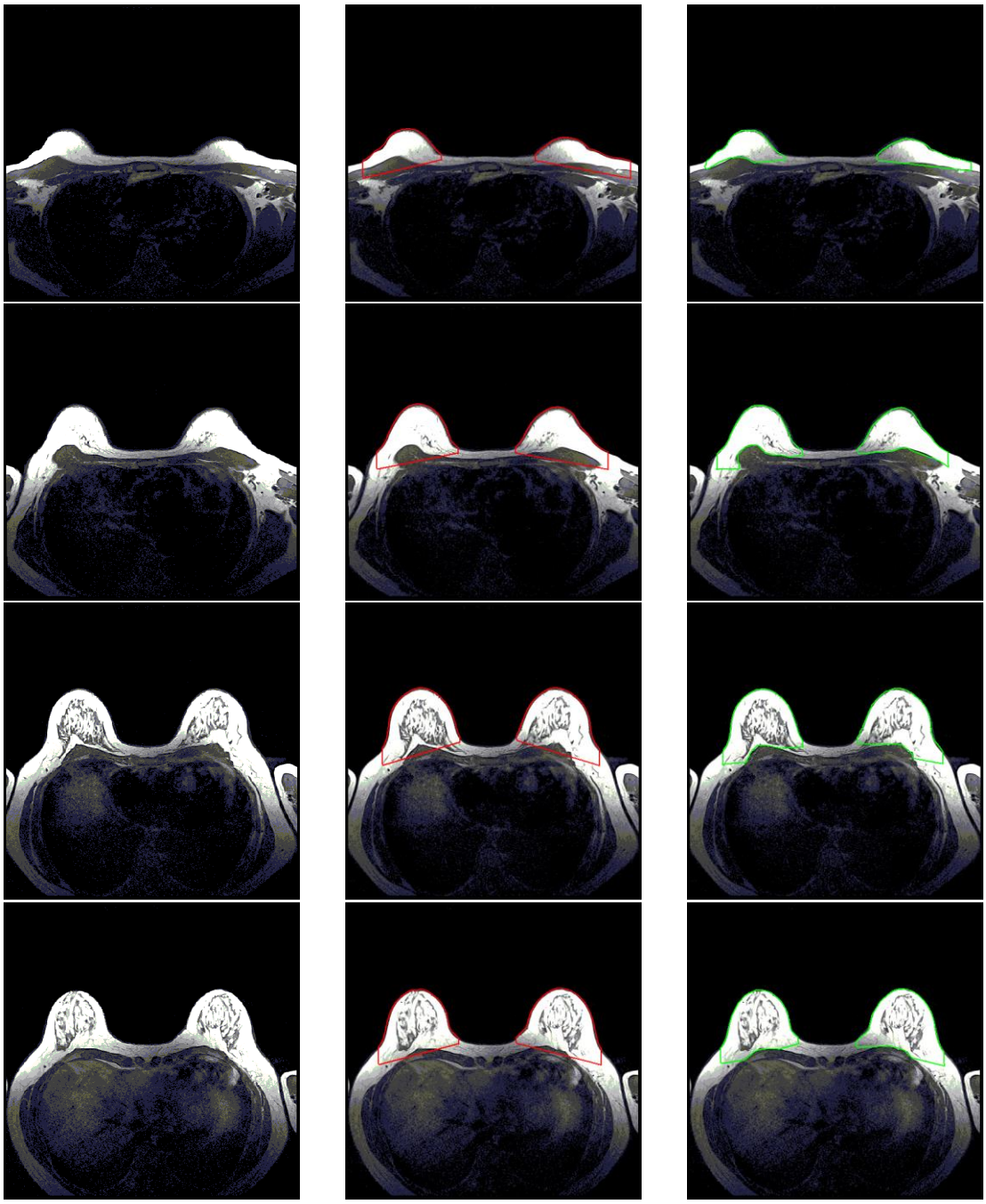

(a) (b) (c)

Figure 3.12: The result of case 11 of proposed method (45 slices per case). (a) The original DICOM images, (b) segmented result, (c) manually sketched result. (Continued)

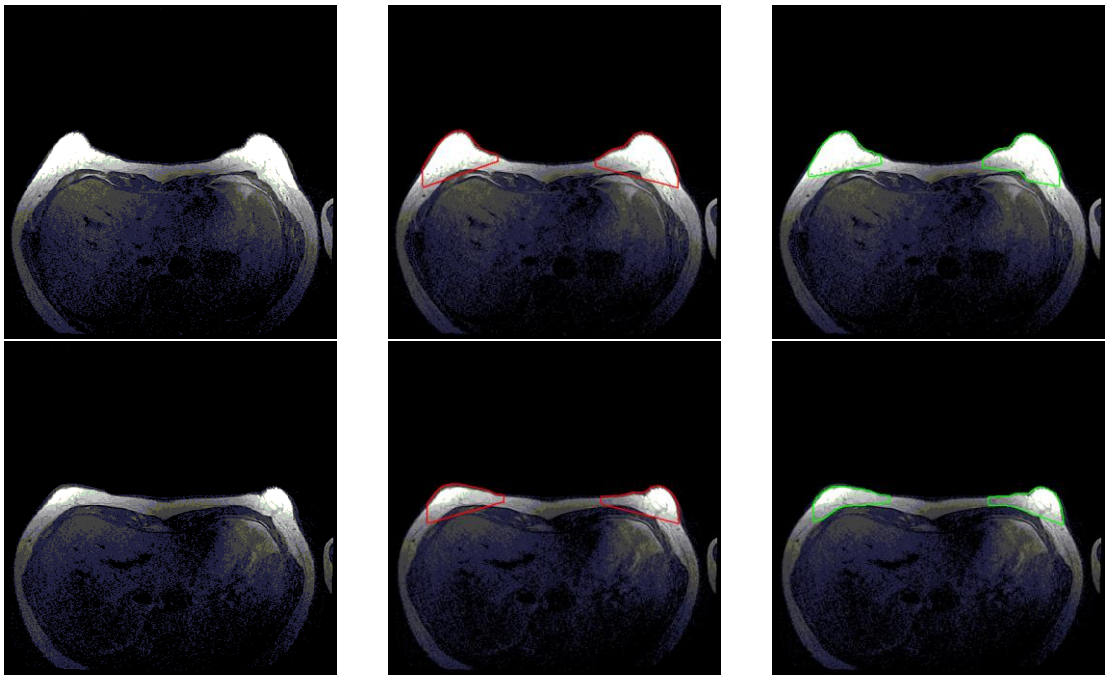

(a) (b) (c)

Figure 3.12: The result of case 11 of proposed method (45 slices per case). (a) The original DICOM images, (b) segmented result, (c) manually sketched result.

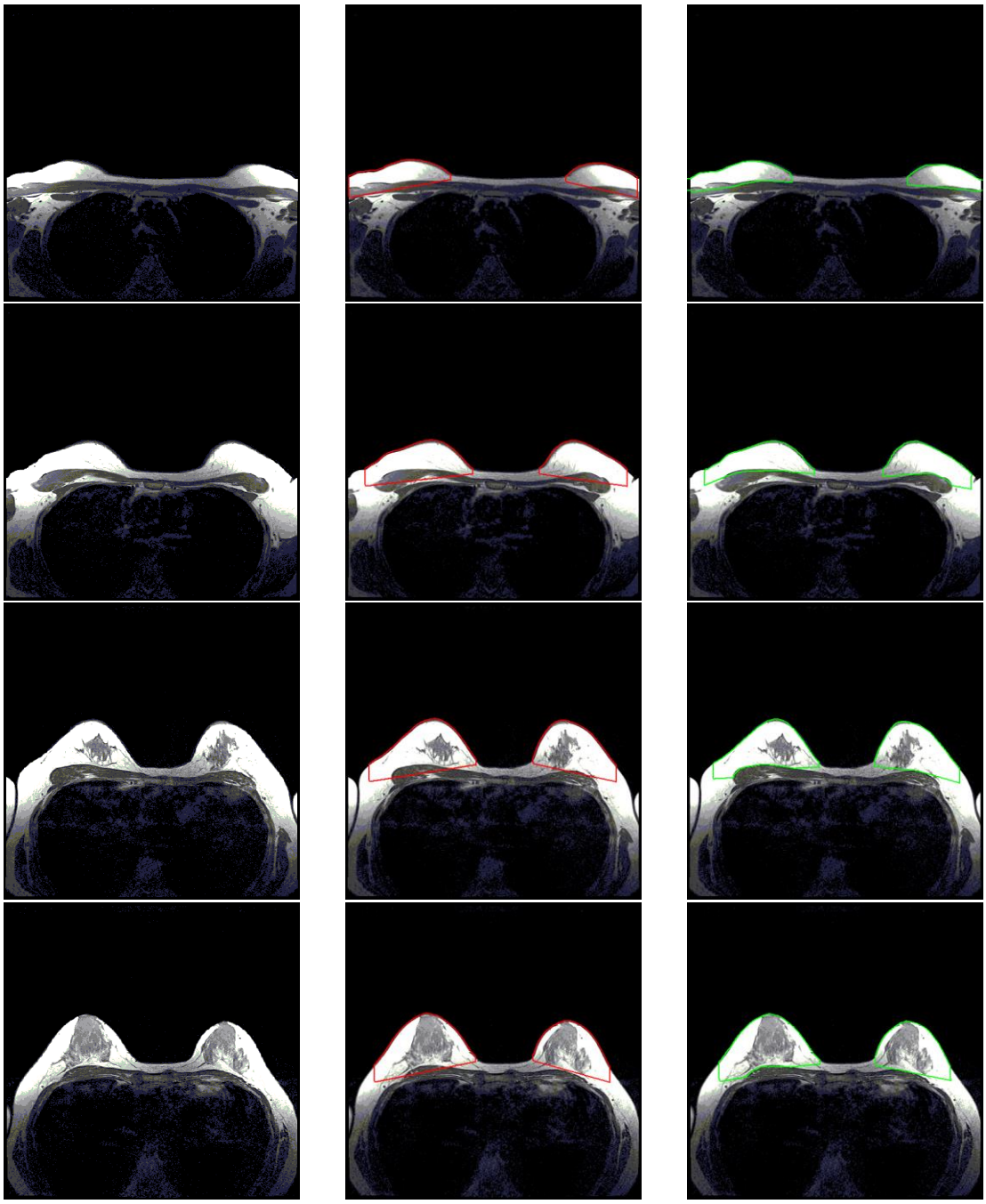

(a) (b) (c)

Figure 3.13: The result of case 12 of proposed method (45 slices per case). (a) The original DICOM images, (b) segmented result, (c) manually sketched result. (Continued)

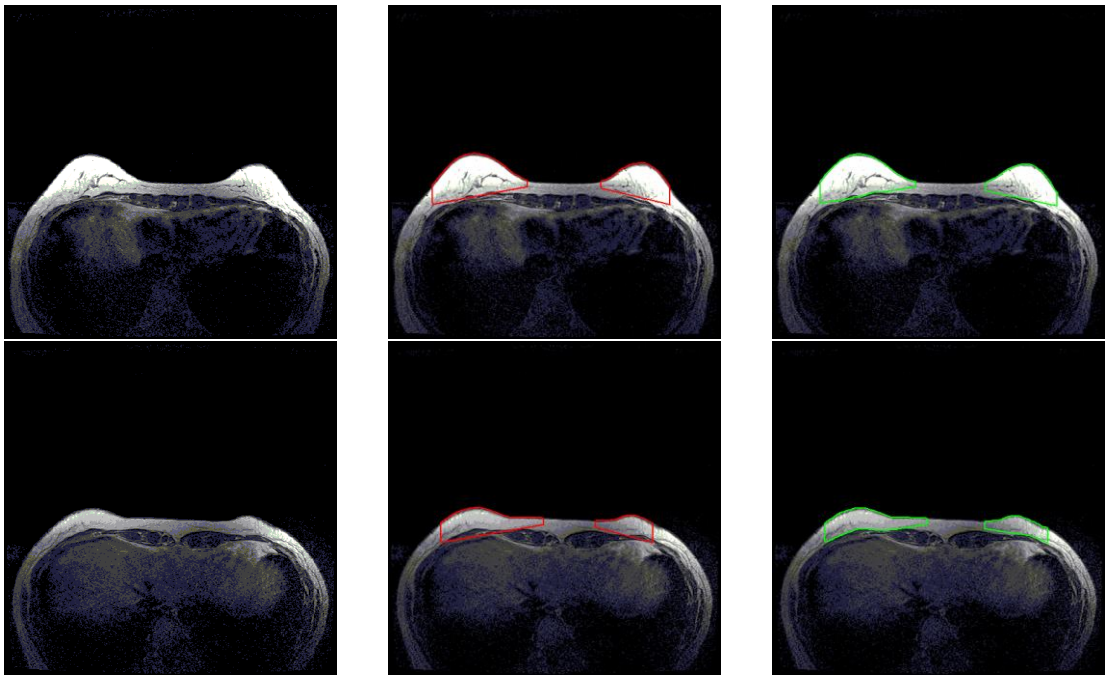

(a) (b) (c)

Figure 3.13: The result of case 12 of proposed method (45 slices per case). (a) The original DICOM images, (b) segmented result, (c) manually sketched result.

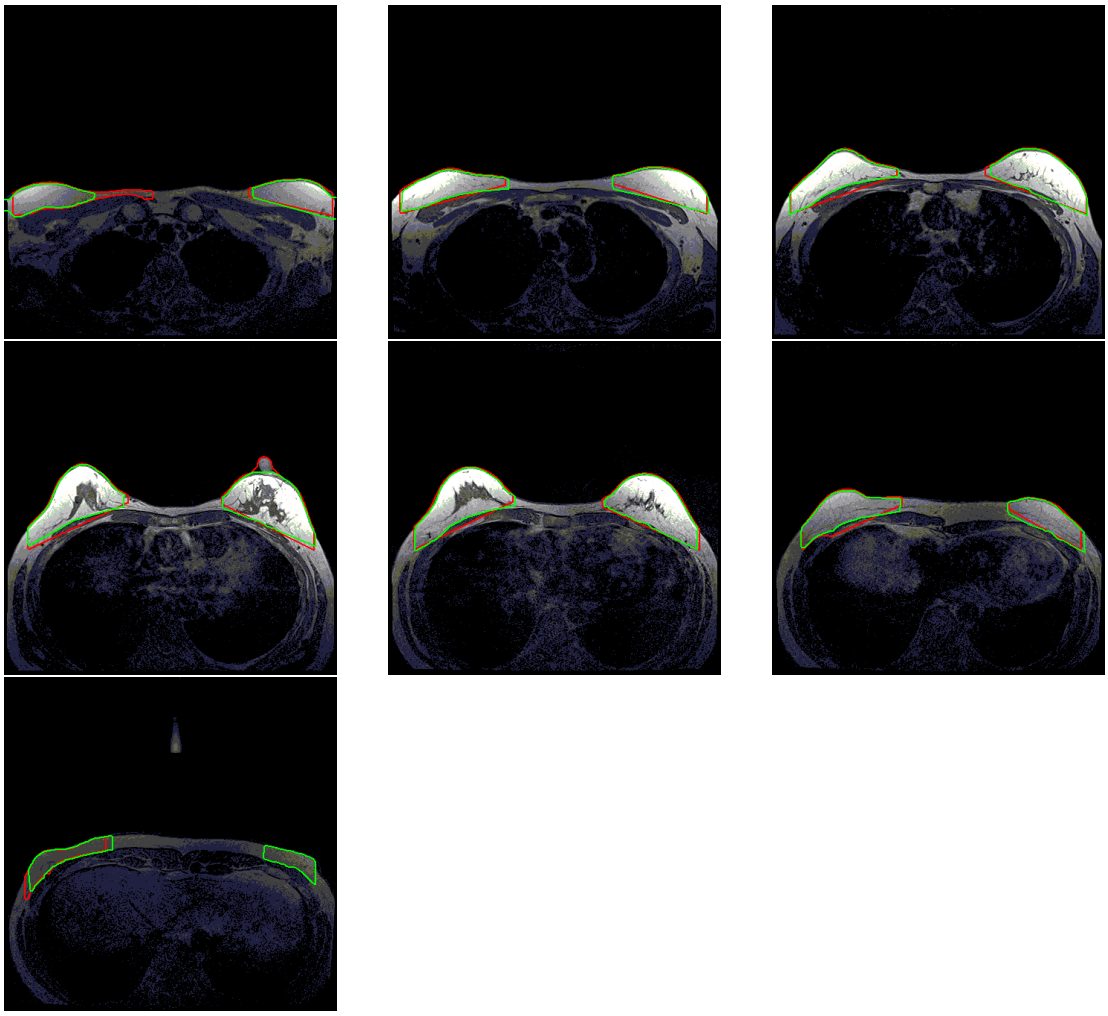

Figure 3.14: The result of case 1 of overlapped the contour determined by our method and physician (60 slices per case): the red contour is result of the proposed method and the green contour is the contour sketched by physician.

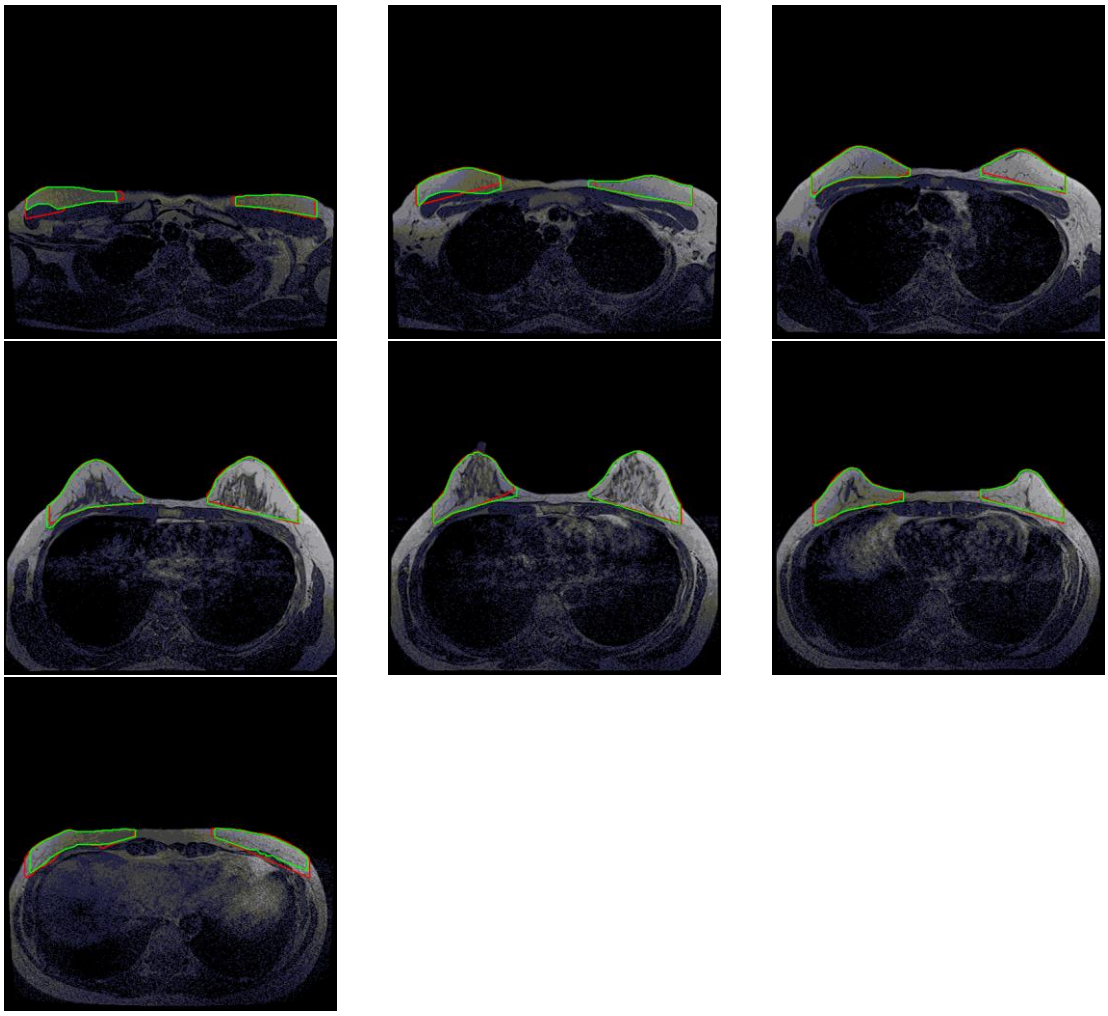

Figure 3.15: The result of case 2 of overlapped the contour determined by our method and physician (60 slices per case): the red contour is result of the proposed method and the green contour is the contour sketched by physician.

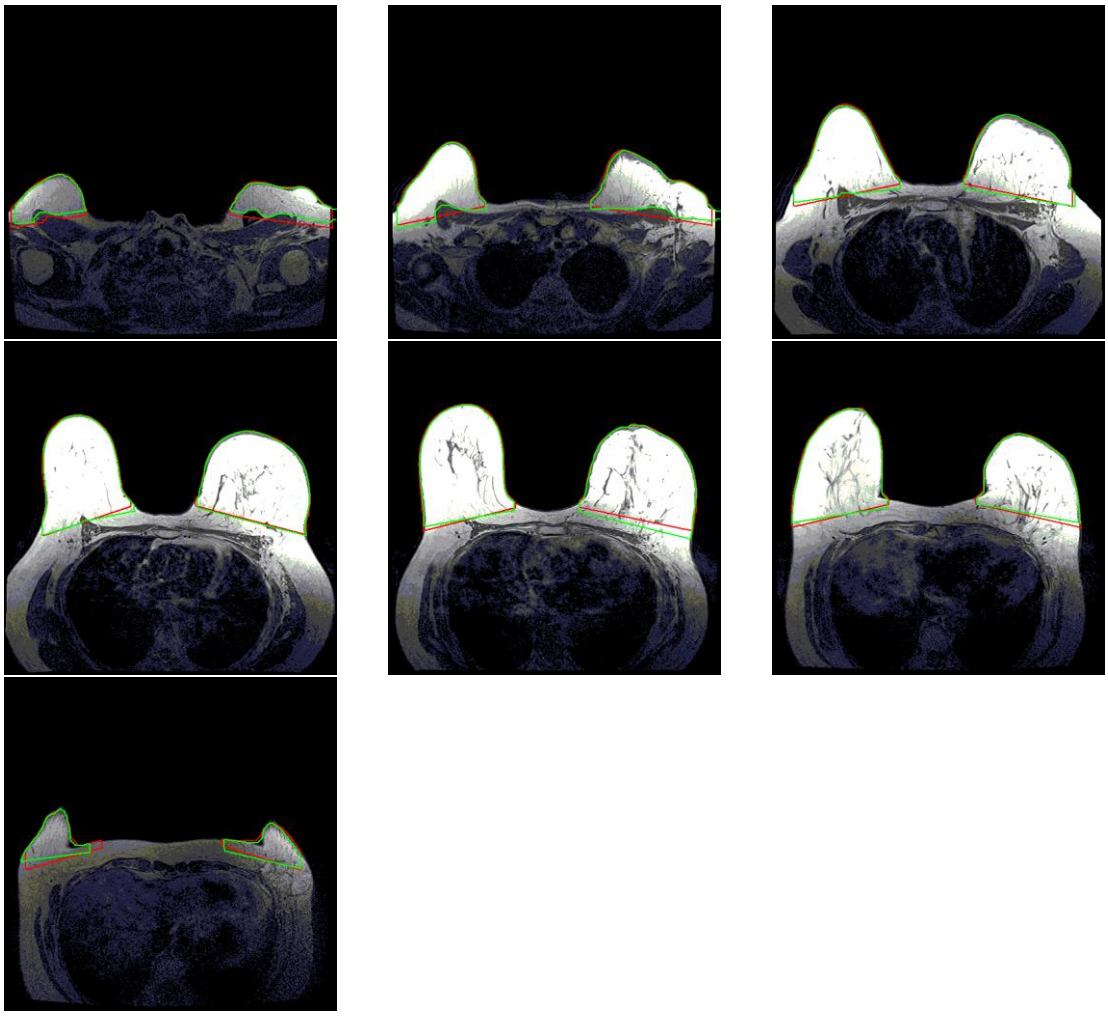

Figure 3.16: The result of case 3 of overlapped the contour determined by our method and physician (60 slices per case): the red contour is result of the proposed method and the green contour is the contour sketched by physician.

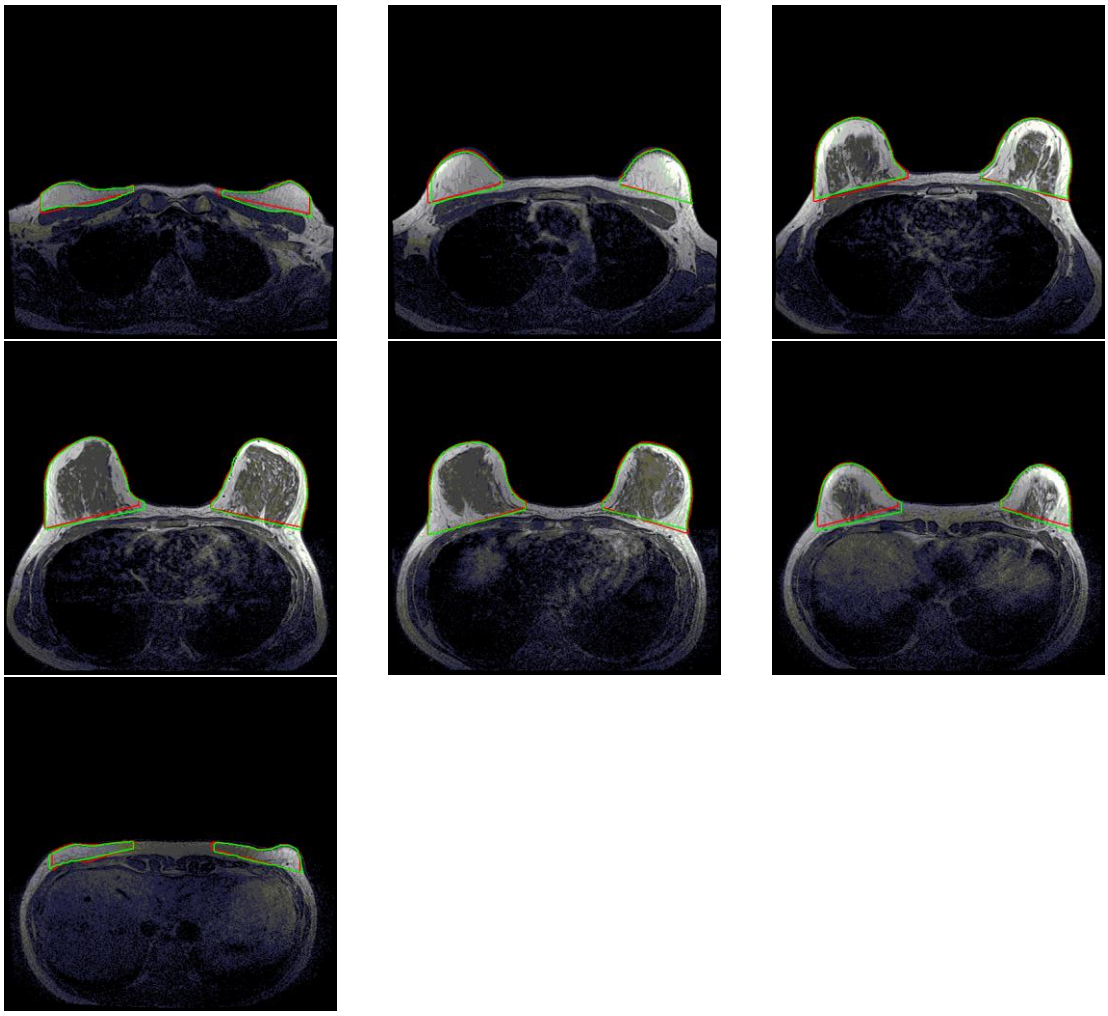

Figure 3.17: The result of case 4 of overlapped the contour determined by our method and physician (60 slices per case): the red contour is result of the proposed method and the green contour is the contour sketched by physician.

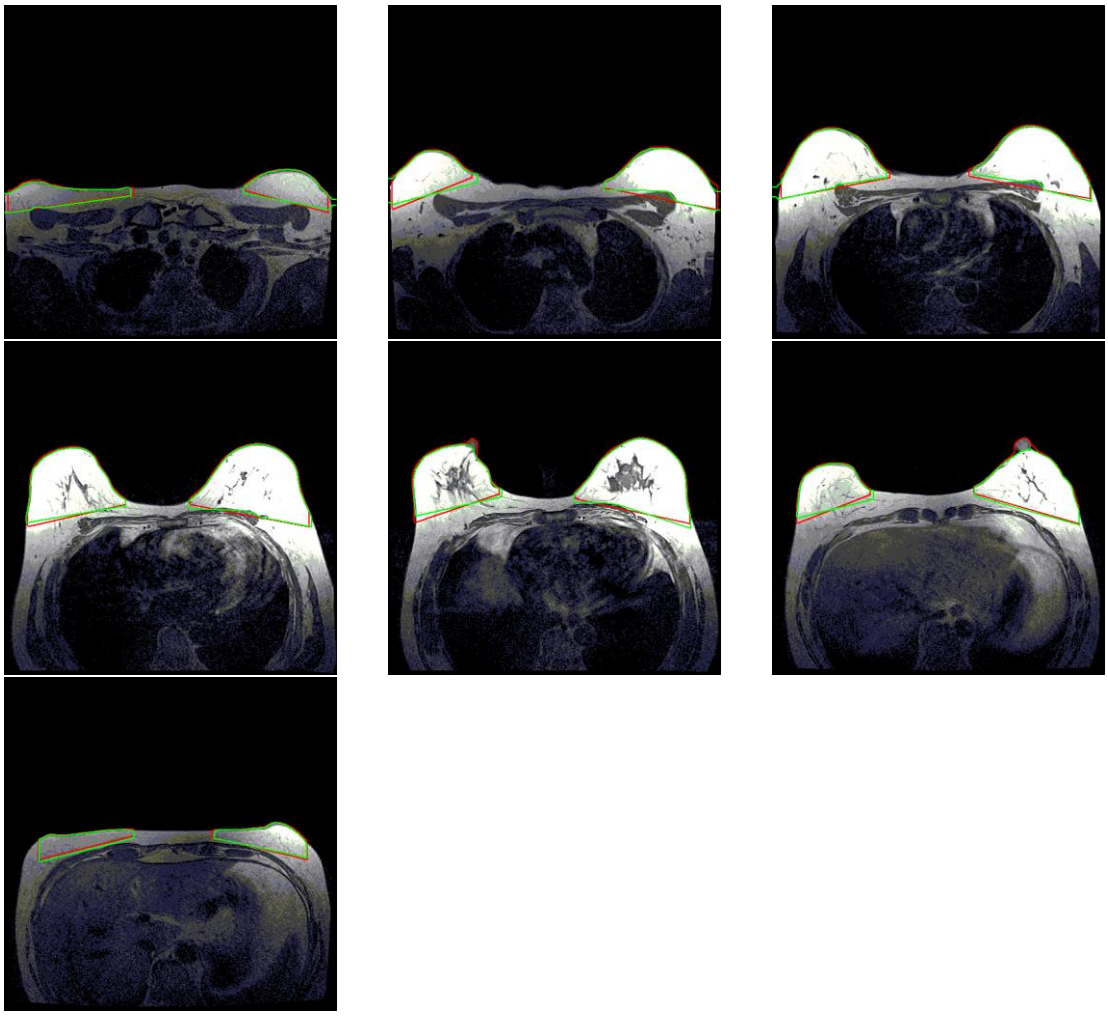

Figure 3.18: The result of case 5 of overlapped the contour determined by our method and physician (60 slices per case): the red contour is result of the proposed method and the green contour is the contour sketched by physician.

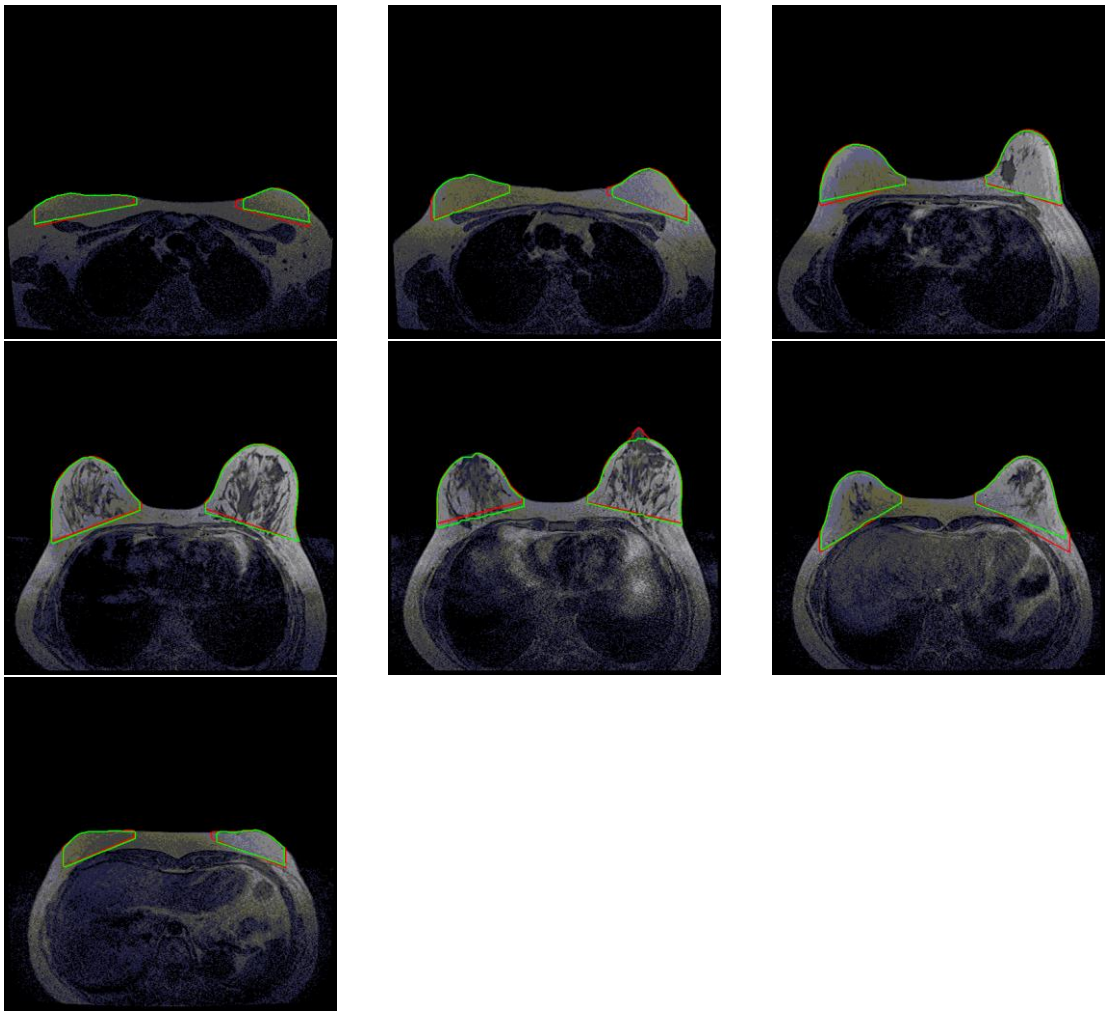

Figure 3.19: The result of case 6 of overlapped the contour determined by our method and physician (60 slices per case): the red contour is result of the proposed method and the green contour is the contour sketched by physician.

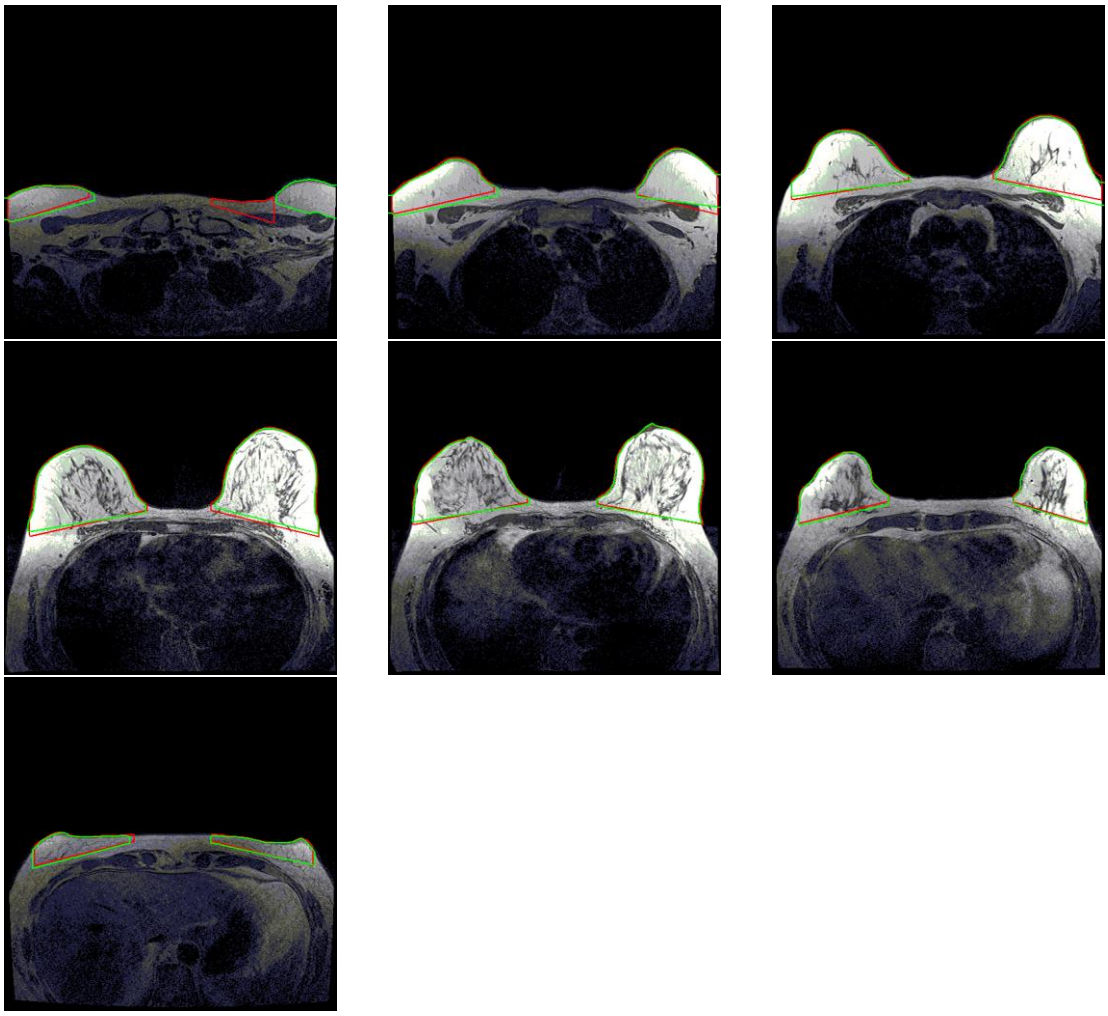

Figure 3.20: The result of case 7 of overlapped the contour determined by our method and physician (60 slices per case): the red contour is result of the proposed method and the green contour is the contour sketched by physician.

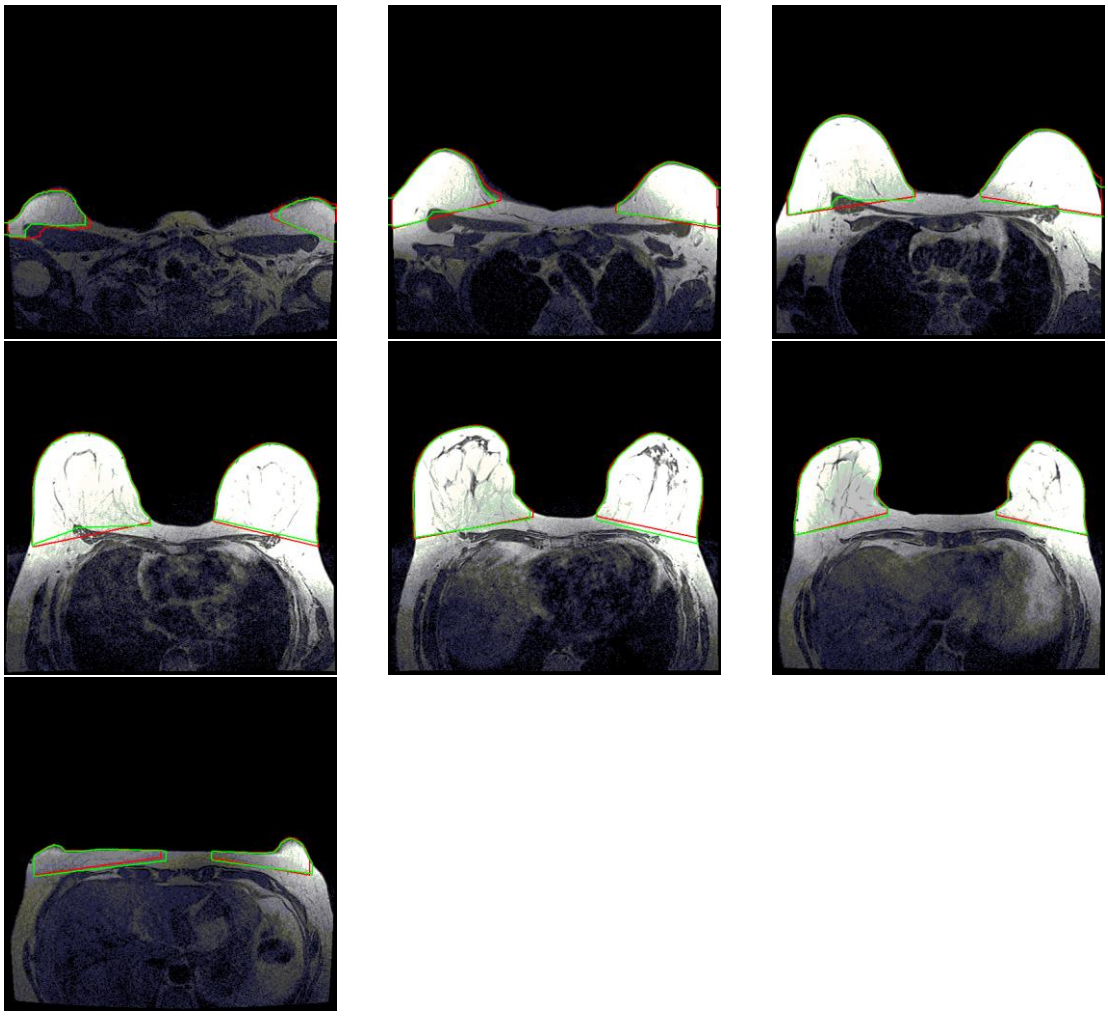

Figure 3.21: The result of case 8 of overlapped the contour determined by our method and physician (60 slices per case): the red contour is result of the proposed method and the green contour is the contour sketched by physician.

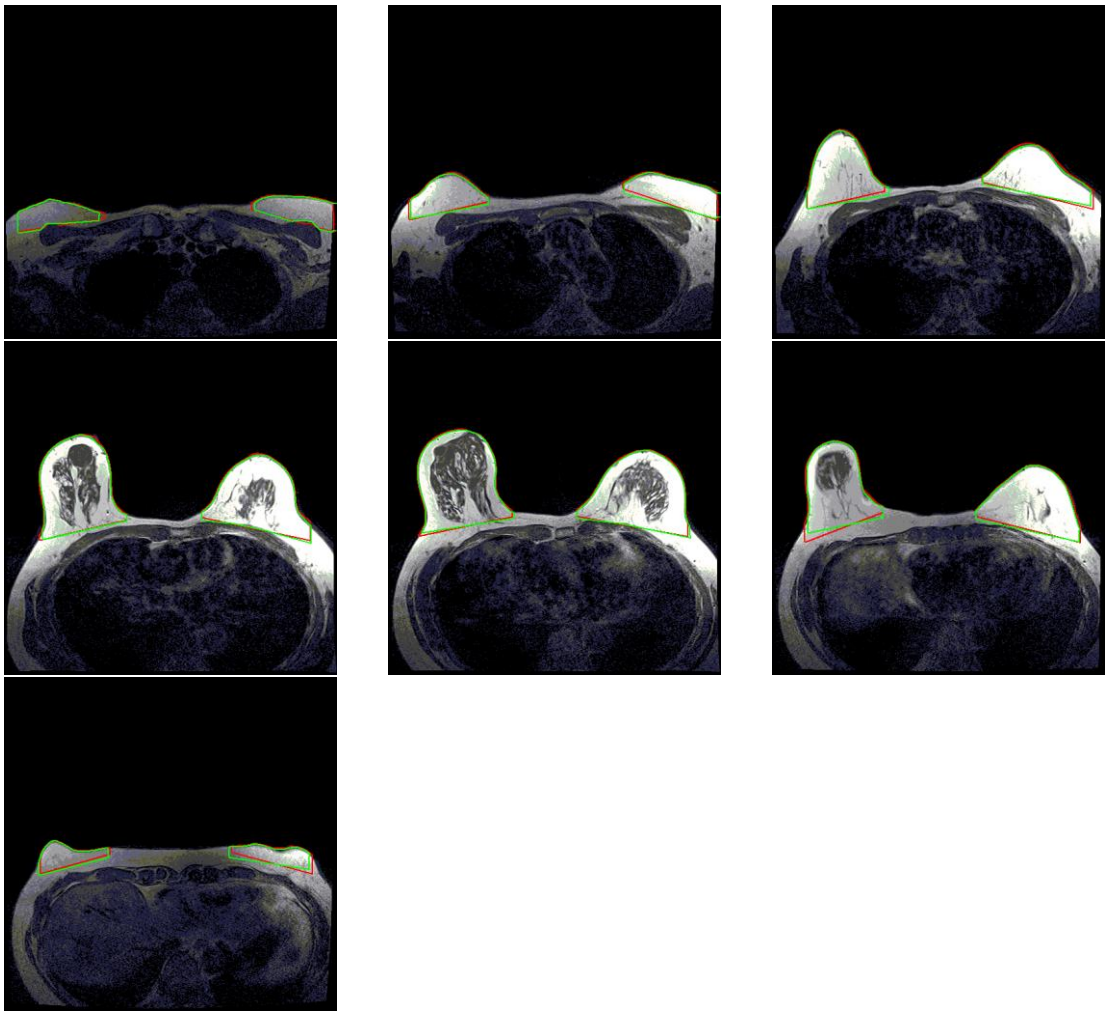

Figure 3.22: The result of case 9 of overlapped the contour determined by our method and physician (60 slices per case): the red contour is result of the proposed method and the green contour is the contour sketched by physician.

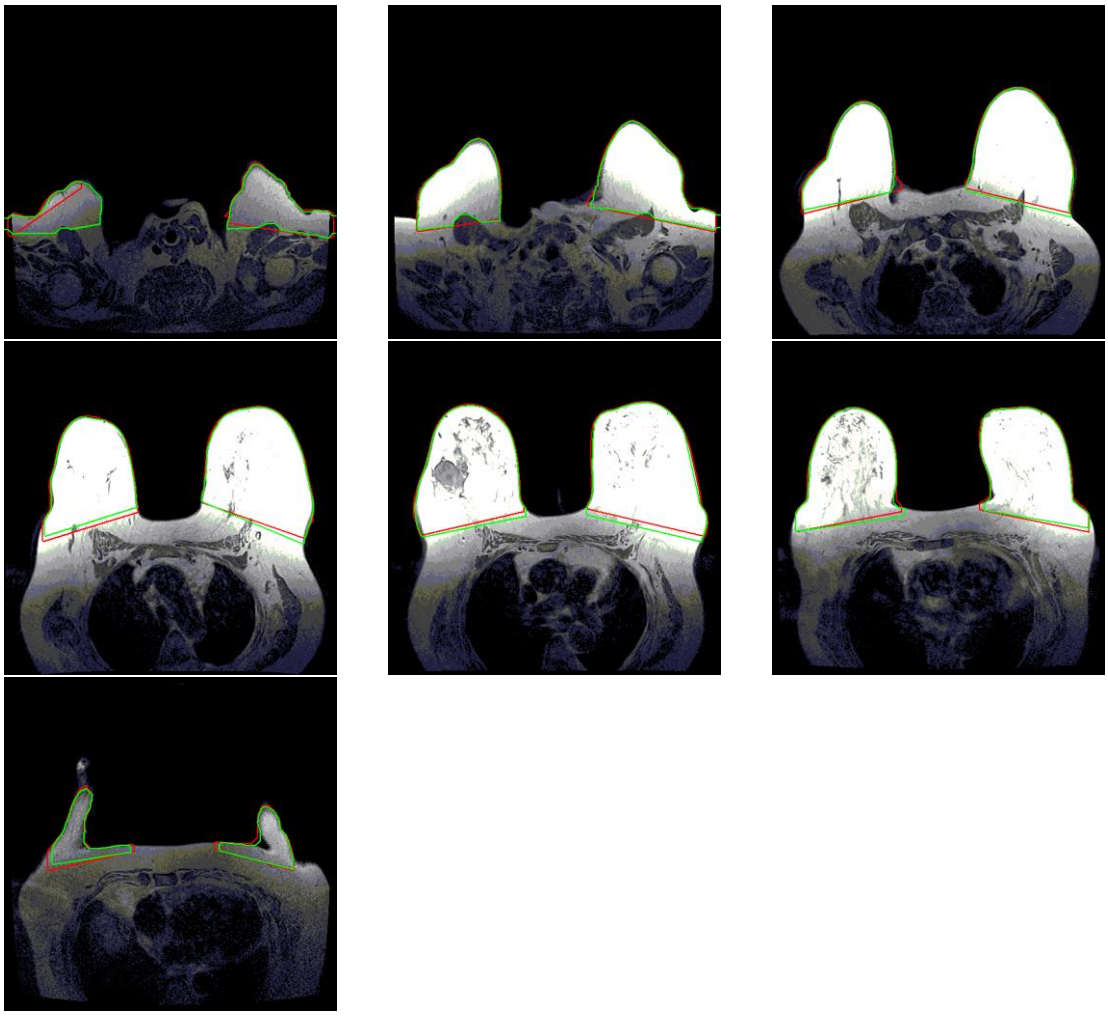

Figure 3.23: The result of case 10 of overlapped the contour determined by our method and physician (60 slices per case): the red contour is result of the proposed method and the green contour is the contour sketched by physician.

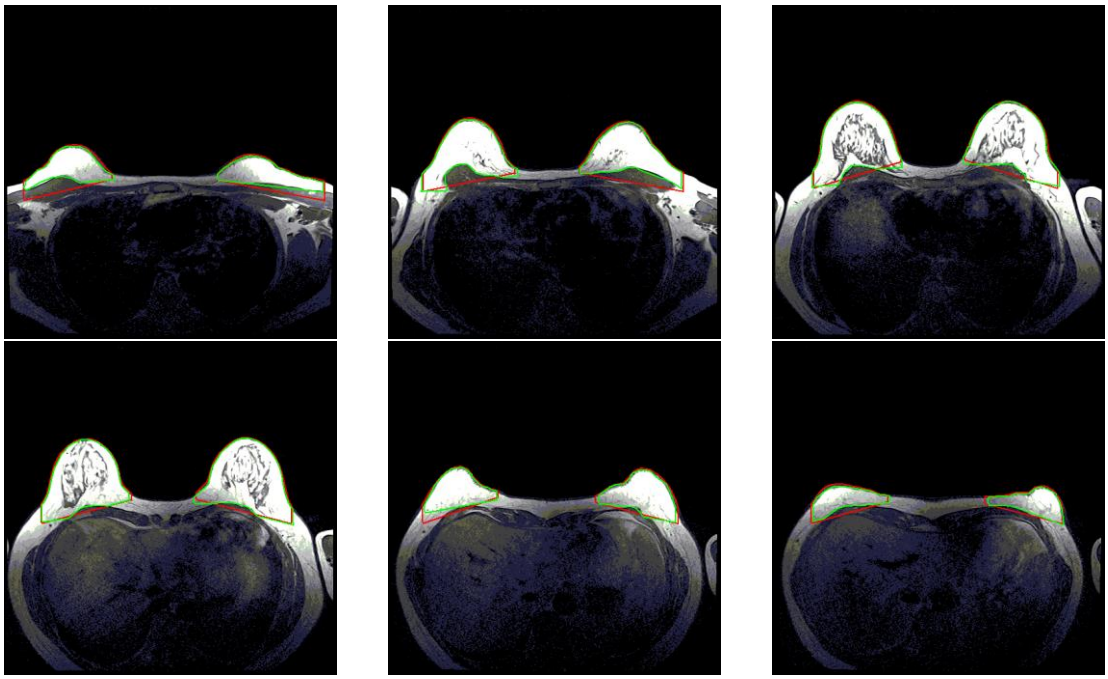

Figure 3.24: The result of case 11 of overlapped the contour determined by our method and physician (45 slices per case): the red contour is result of the proposed method and the green contour is the contour sketched by physician.

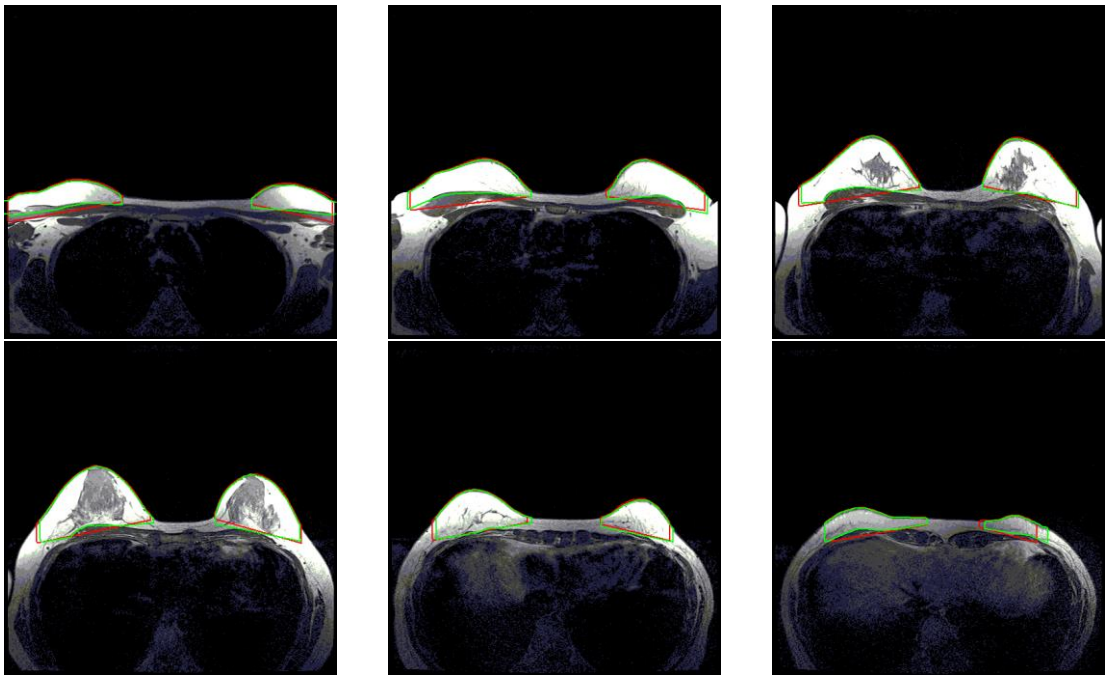

Figure 3.25: The result of case 12 of overlapped the contour determined by our method and physician (45 slices per case): the red contour is result of the proposed method and the green contour is the contour sketched by physician.

Table 3.1: The four similarity measures of all cases.

Case no.	SI	OF	OV	EF
1	0.91	0.88	0.84	0.17
2	0.93	0.91	0.88	0.12
3	0.94	0.93	0.90	0.10
4	0.94	0.94	0.90	0.10
5	0.94	0.92	0.89	0.10
6	0.95	0.95	0.91	0.08
7	0.94	0.93	0.90	0.10
8	0.95	0.94	0.91	0.08
9	0.94	0.94	0.90	0.10
10	0.95	0.95	0.91	0.09
11	0.91	0.85	0.84	0.16
12	0.91	0.86	0.84	0.16
Average	0.94	0.92	0.88	0.11

SI: similarity index; OF: over fraction; OV: over value; EF: extra fraction

CHAPTER 4

Discussion and Conclusions

Nowadays, there are many modalities for detecting breast cancer, the benefit of MRI are high sensitivity to the nidus of breast tissues, non-invasive, multi-view images and non-radioactive. Thus breast MRI become more widespread used. In recent year, the rapid development of computer technology, CAD system is used in diagnosis more popularly than before.

This study demonstrate an efficient and rapidly method to detect contours of breast region on MRI. This work could reduce the wrong decision by the radiologist who is inexperienced. The proposed method uses thresholding method, anisotropic filter and morphological processing as the pre-processing procedure to decrease the noises and retain the shape of the breast. The segmentation method based on the projection techniques is performed to distinguish breast region from other tissues. The contours determined by the proposed method achieves the high similarity to manual sketched contours. The proposed segmentation method is valuable for physicians to make decision during the operation.

The performance analysis is examined by for practical similarity measures in Table 4.1. The average *SI* reaches 0.94 and the average *EF* is 0.11. It means that the segmentation method proposed by this study is outstanding and trustworthy. According to the experiment of 12 cases, it shows several advantages of the proposed method: (1) The proposed algorithm is adaptive to every case. User don’t need to revise any parameter. (2) It is easy for user without any anatomy or pathology process. User just need to select the series of MR images and the breast region area could be computed by system. (3) It is an efficient algorithm. The computation time for the whole

segmentation of one case only take within 30 second, including pre-processing and depicting the breast contour. To summarize those superiorities, the result shows high potential to be necessary in computer-aided analysis systems. Besides, the segmentation result is confirmed by physicians that is valuable for not only the breast augmentation surgery but the breast cancer research.

However, the improvements are still required. The performance of a few cases was unsatisfied. In Fig. 4.1, the proposed system obtained an unsatisfied result of the breast region because of the insufficient contrast. In Fig. 4.2, these cases are segmented at the incorrect position due to the parameters that are consistent in all cases. The proposed method would be fine adjust to assure the accuracy of the horizontal and vertical projection segmentation to avoid the boundary of the breast being in correct position. In the nearly future, we may improve our approach to reach the goal of extracting the fibro-glandular tissue and emphasize the region of tumor. We believe that the proposed method could be used in clinical breast reconstruction operation.

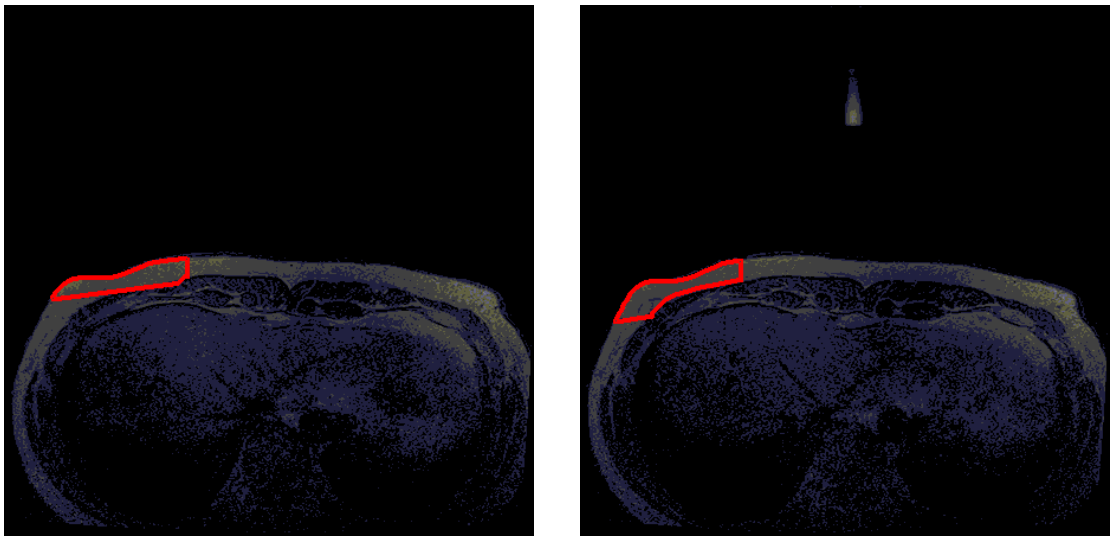

Figure 4.1: The defected results by the proposed method

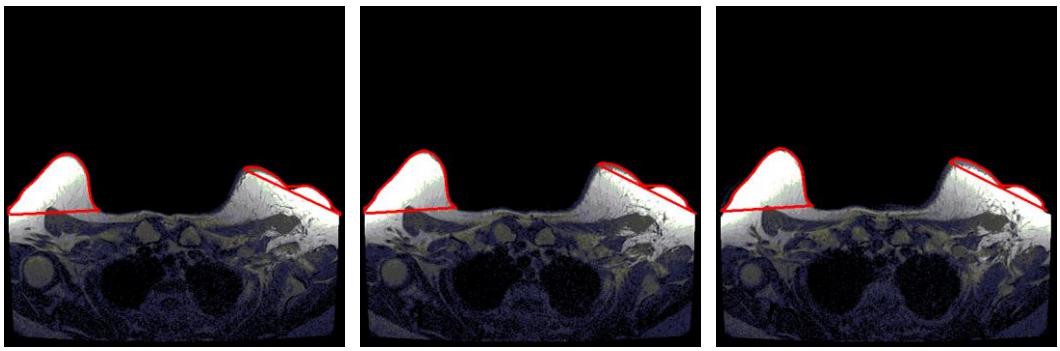

Figure 4.2: The defected results by the proposed method

Table 4.1: The average of four similarity measures of all cases.

Four average measures				
	SI	OF	OV	EF
Value	0.94	0.92	0.88	0.11

SI: similarity index; OF: over fraction; OV: over value; EF: extra fraction

References

[1] A. C. Society, "Breast Cancer Facts and Figures 2015-2016.," 2016.

[2] T. Berber, A. Alpkocak, P. Balci, and O. Dicle, "Breast mass contour segmentation algorithm in digital mammograms," *Computer methods and programs in biomedicine,* vol. 110, pp. 150-159, 2013.

[3] S. Ribes, D. Didierlaurent, N. Decoster, E. Gonneau, L. Risser, V. Feillel, *et al.*, "Automatic segmentation of breast MR images through a Markov random field statistical model," *Medical Imaging, IEEE Transactions on,* vol. 33, pp. 1986-1996, 2014.

[4] S. H. Lewis and A. Dong, "Detection of breast tumor candidates using marker-controlled watershed segmentation and morphological analysis," in *Image Analysis and Interpretation (SSIAI), 2012 IEEE Southwest Symposium on*, 2012, pp. 1-4.

[5] P. Gu, W.-M. Lee, M. A. Roubidoux, J. Yuan, X. Wang, and P. L. Carson, "Automated 3D ultrasound image segmentation to aid breast cancer image interpretation," *Ultrasonics,* vol. 65, pp. 51-58, 2016.

[6] H. H. Aghdam, D. Puig, and A. Solanas, "Adaptive Probabilistic Thresholding Method for Accurate Breast Region Segmentation in Mammograms," in *2014 22nd International Conference on Pattern Recognition (ICPR)*, 2014, pp. 3357-3362.

[7] G. k. ErtaE , GC, O. Osman, O. N. UC'an, M. TunacD1, and M. Dursun, "Breast MR segmentation and lesion detection with cellular neural networks and 3D template matching," *Computers in biology and medicine,* vol. 38, pp. 116-126, 2008.

[8] A. Gumaei, A. El-Zaart, M. Hussien, and M. Berbar, "Breast segmentation using

k-means algorithm with a mixture of gamma distributions," in *Broadband Networks and Fast Internet (RELABIRA), 2012 Symposium on*, 2012, pp. 97-102.

[9] M. Mustra and M. Grgic, "Robust automatic breast and pectoral muscle segmentation from scanned mammograms," *Signal processing*, vol. 93, pp. 2817-2827, 2013.

[10] J. A. Martinez-Mera, P. G. Tahoces, J. M. Carreira, J. J. Suarez-Cuenca, and M. Souto, "A hybrid method based on level set and 3D region growing for segmentation of the thoracic aorta," *Computer Aided Surgery*, vol. 18, pp. 109-117, 2013.

[11] R. Adams and L. Bischof, "Seeded Region Growing," *Ieee Transactions on Pattern Analysis and Machine Intelligence*, vol. 16, pp. 641-647, Jun 1994.

[12] S. Wu, S. P. Weinstein, E. F. Conant, M. D. Schnall, and D. Kontos, "Automated chest wall line detection for whole-breast segmentation in sagittal breast MR images," *Medical physics*, vol. 40, p. 042301, 2013.

[13] M. Lin, J.-H. Chen, X. Wang, S. Chan, S. Chen, and M.-Y. Su, "Template-based automatic breast segmentation on MRI by excluding the chest region," *Medical physics*, vol. 40, p. 122301, 2013.

[14] M. Sezgin, "Survey over image thresholding techniques and quantitative performance evaluation," *Journal of Electronic imaging*, vol. 13, pp. 146-168, 2004.

[15] K. Wu and D. Zhang, "Robust tongue segmentation by fusing region-based and edge-based approaches," *Expert Systems with Applications*, vol. 42, pp. 8027-8038, 2015.

[16] L. Wang and C. Pan, "Robust level set image segmentation via a local correntropy-based K-means clustering," *Pattern Recognition*, vol. 47, pp. 1917-1925, 2014.

[17] R. C. Gonzalez and R. E. Woods, "Digital Image Processing 3nd Edition," *Chapter 10.4 Region Growing Segmentation,* pp. 763-769, 2008.

[18] J. Canny, "A computational approach to edge detection," *IEEE Trans Pattern Anal Mach Intell,* vol. 8, pp. 679-698, Jun 1986.

[19] H. I. Works, "Sobel Edge Detector."

[20] N. Otsu, "Threshold Selection Method from Gray-Level Histograms," *IEEE Transactions on Systems Man and Cybernetics,* vol. 9, pp. 62-66, 1979.

[21] A. Fooladivanda, S. B. Shokouhi, N. Ahmadinejad, and M. R. Mosavi, "Automatic segmentation of breast and fibroglandular tissue in breast MRI using local adaptive thresholding," in *Biomedical Engineering (ICBME), 2014 21th Iranian Conference on*, 2014, pp. 195-200.

[22] L. Wang, B. Platel, T. Ivanovskaya, M. Harz, and H. K. Hahn, "Fully automatic breast segmentation in 3D breast MRI," in *Biomedical Imaging (ISBI), 2012 9th IEEE International Symposium on*, 2012, pp. 1024-1027.

[23] J. A. Rosado-Toro, T. Barr, J.-P. Galons, M. T. Marron, A. Stopeck, C. Thomson, *et al.*, "Automated segmentation of breast fat-water MR images using empirical analysis," in *Acoustics, Speech and Signal Processing (ICASSP), 2013 IEEE International Conference on*, 2013, pp. 1018-1022.

[24] S. K. Swee, C. F. Keong, C. S. Siang, T. C. Peng, S. F. Abbas, and S. Omar, "Projection Based Region of Interest Segmentation in Breast MRI Images," *International Journal on Advanced Science, Engineering and Information Technology,* vol. 1, pp. 113-116, 2011.

[25] J. MilenkoviD , O. Chambers, M. M. MuE!iD , and J. F. TasiD "Automated breast-region segmentation in the axial breast MR images," *Computers in biology and medicine,* vol. 62, pp. 55-64, 2015.

[26] P. Perona and J. Malik, "Scale-space and edge detection using anisotropic

diffusion," *Pattern Analysis and Machine Intelligence, IEEE Transactions on,* vol. 12, pp. 629-639, 1990.

[27] R. Rouhi, M. Jafari, S. Kasaei, and P. Keshavarzian, "Benign and malignant breast tumors classification based on region growing and CNN segmentation," *Expert Systems with Applications,* vol. 42, pp. 990-1002, 2015.

[28] Y. Tan, L. Liu, Q. Liu, J. Wang, X. Ma, and H. Ni, "Automatic breast DCE-MRI segmentation using compound morphological operations," in *Biomedical Engineering and Informatics (BMEI), 2011 4th International Conference on*, 2011, pp. 147-150.

[29] A. Gubern-MC)rida, M. Kallenberg, R. M. Mann, R. Marti, and N. Karssemeijer, "Breast segmentation and density estimation in breast MRI: a fully automatic framework," *Biomedical and Health Informatics, IEEE Journal of,* vol. 19, pp. 349-357, 2015.

[30] P. Anbeek, K. L. Vincken, M. J. van Osch, R. H. Bisschops, and J. van der Grond, "Probabilistic segmentation of white matter lesions in MR imaging," *NeuroImage,* vol. 21, pp. 1037-1044, 2004.